

INTER-AMERICAN TROPICAL TUNA COMMISSION

SCIENTIFIC ADVISORY COMMITTEE

14TH MEETING

La Jolla, California (USA)

15-19 May 2023

DOCUMENT SAC-14-06

**YELLOWFIN TUNA STOCK ASSESSMENT: CONCEPTUAL MODEL AND
EXPLORATORY ANALYSES**

Carolina Minte-Vera, Mark N. Maunder, Haikun Xu, Cleridy E. Lennert-Cody, Jon Lopes, Alexandre Aires-da-Silva, Daniel W. Fuller, Mitchell S. Lovell

CONTENTS

ABSTRACT.....	2
Introduction	2
Spatial structure of yellowfin tuna in the eastern Pacific Ocean.....	3
Update of the conceptual model for yellowfin tuna in the EPO.....	5
Molecular studies.....	6
Larval distribution and reproductive biology.....	7
Dynamic boundaries and mixing.....	9
Tagging data	11
Dynamic discrimination of stocks	13
Principal component analysis on oceanographic variables	13
Tree analysis of length composition data	14
Stock separation	20
Population trends and dynamics	22
Catches.....	26
Discussion	28
Future directions.....	31
References	32
Appendix A. Principal Component analysis on oceanographic variables	35
Appendix B. regression Tree analysis on length-frequency data.....	37
Appendix C. Spatiotemporal models for CPUE standardization	38
C1. Standardization procedure	38

ABSTRACT

A conceptual model for yellowfin tuna in the eastern Pacific Ocean (EPO) was refined based on a review of all available information, including information relevant to stock structure. The main component of the updated conceptual model is the idea that there are at least two stocks of yellowfin tuna in the EPO associated with different biogeochemical provinces, epipelagic and mesopelagic, which is supported by a suite of information. The distribution of these two stocks varies seasonally and interannually following the expansion and contraction of the biogeochemical provinces. The main challenges that this pattern poses to stock assessment is to determine where to place the boundary among stocks and how to estimate mixing rates. The dynamic shape of the biogeochemical provinces can be summarized using oceanographic variables, which allows a path forward to delimit the preferred habitat of each stock. Here, we summarized the biogeochemical characteristics of the locations of each purse-seine set from 2000-2017 using principal component analysis. The first component (PC1) summarized the vertical structuring of the water column, while the second component (PC2) mainly represented the sea surface temperature (SST). Tree analyses were used to split the length composition of purse-seine fleet, where the two principal components (a proxy for the location within the environmental gradients) and seasons (quarters and cyclical quarters) were used as explanatory variables. The length frequency data from the purse-seine sets on floating objects was used because it has the largest proportion of smaller and younger fish, that are more likely to inhabit the shallower parts of the water column, thus may be a better indicator of fish originating in each location. The tree analysis showed the first split on the PC2, separating the areas with lower SST (areas of influence of the Humboldt and California currents) from the warmer tropical areas. When the colder areas were removed, the tree analyses on the tropical areas split the length composition along PC1 axis, into two distinct areas, a northeastern (NE) area with lower seas surface height, shallow thermocline and shallow upper layer of the mesopelagic zone, and a southwestern (SW) area with higher sea surface height, deeper thermocline, and deeper upper layer of the mesopelagic zones. The locations of those areas vary seasonally and interannually. The location of the dynamic split is consistent with the conceptual model. The catches were split between the two stocks according to the membership defined by the tree analysis. A pragmatic decision of allocating the colder areas according to their position in the PC1 axis was made. The NE putative stock encompasses almost all the purse-seine catches in weight on dolphins sets, 96% on unassociated sets and 83% of floating objects, while only 17% of the longline catch in numbers (average for 1995-2017). The SW putative stock, in contrast, encompasses 79% of the longline catches and 17% of the floating object catches, with an increase in that proportion in recent years. These analyses will be used as bases to structure models that will be included in the risk analysis for the 2024 Benchmark Assessment.

INTRODUCTION

The models used to assess yellowfin tuna in the EPO are statistical catch-at-age models and are built using the paradigm of integrated analysis, which allows the model to be fit simultaneously to a wide array of data (Maunder and Punt, 2013). Frequently data components may seem to have contradictory information, which is most likely created by a mis-specified model that is not an adequate representation of the system. Solving model misspecification should reconcile the apparently inconsistent information from the data. In some cases, despite the best efforts of the analyst, the misspecification cannot be resolved. This was the case for the yellowfin tuna assessment in the EPO.

In 2019, the yellowfin tuna assessment was rejected based on the results being too sensitive to the main index of abundance, which was derived from the Japanese longline catch per unit of effort (CPUE) data. Secondary indices derived from the CPUE of the purse-seine data were used in the assessment and showed patterns that were divergent from the longline index. Modifications of the methods for estimating

the indices of abundance (which were delta-lognormal models for the longline index or nominal CPUE for the purse-seine indices at the time) were done and new models were constructed using the state-of-the-art spatiotemporal models (Xu et al 2019, Maunder et al 2020), but the discrepancies between the indices persisted ([SAC-10-Inf-F](#)). We hypothesized that the discrepancies between the two indices may be due to spatial structure. Attempts to address the spatial structure were done in preparation for the external review of the yellowfin tuna assessment ([YFT-02](#)), but the review panel concluded that although spatial structure seem to be the cause of the discrepant patterns, there was more research and consideration needed to be able to split the areas ([YFT-02-Rep](#)).

In the 2020 benchmark assessment for yellowfin tuna ([SAC-11-07](#)), a risk analysis approach was adopted ([SAC-10-INF-J](#)). The risk analysis encompassed a suite of models that reflected hypotheses about the population dynamics (organized in a hierarchical way), which are collectively a conceptual model for the stock. The overarching hypothesis for yellowfin tuna was that at least two groups with distinct dynamics (two stock, or two sub-stocks) are present in the EPO. A set of nested hypotheses regarding the degree of mixing of those two groups was proposed. At the time, a pragmatic approach was adopted to assess the yellowfin tuna stock of focusing on the core of the catches and evaluating the hypothesis of high mixing, while assuming the purse-seine index as reliable and the longline index as unreliable for representing the population trends. The alternative hypotheses, which considered heterogenous population structure, were not evaluated as more research is needed. For the 2024 benchmark assessment, it is expected that those hypotheses be evaluated as well.

In this document, we review all available information and update the conceptual model (CM) for yellowfin tuna in the EPO updated. The evidence for the existence of at least two genetically distinct stocks of yellowfin tuna was summarized. The CM is internally coherent and able to explain the discrepancies among the purse-seine and longline indices of abundance. We also propose a methodology to split between the two stocks that is based on hypotheses about the association of the two stock with marine biogeochemical provinces and exploratory data analysis of length-composition data. The catches for 2000-2017 are allocated between the two stocks. We discuss the implications of the findings for the design of new models to be included in the risk analysis of the yellowfin tuna stock for the 2024 benchmark assessment.

SPATIAL STRUCTURE OF YELLOWFIN TUNA IN THE EASTERN PACIFIC OCEAN

During the development of fisheries for yellowfin tuna in the EPO, the fleets expanded over time in two directions: the purse-seine fisheries expanded from the coast to offshore while the industrial longline fisheries did the opposite and expanded from the central Pacific Ocean (CPO) to the EPO. The early days of the coastal fishery were conducted using pole and line, which was introduced in the early 1900s by Japanese immigrants in San Diego, California (Estes 1983). At the peak of the pole-and-line fishery, in the mid- to late-1950s, the fleet operated from California to northern Peru, always in areas relatively close to the coast. By the 1960s, the larger pole-and-line vessels were converted to purse seiners. As the conversions progressed and as new purse-seine vessels entered the fleet, the pole-and-line fishery waned, and the purse-seine fishery expanded to regions considerably further offshore. In the 1950s, the Japanese longline fleet started operating in the EPO expanding their operations from the western/central Pacific Ocean to the coast of the Americas in the early 1960s, followed by the Korean and Chinese Taipei longline fleets in the 1970s.

Only one yellowfin stock has been assumed to be present the EPO since the creation of the Inter-American Tropical Tuna Commission (IATTC) in 1949. In the 1980s, the assessments were done, based exclusively on the purse-seine fisheries, using cohort analysis, which used the length composition data to estimate the catch-at-age (Tomlinson unpublished manuscript). Spatial structure at the fisheries level was

introduced in 2000 by using the “areas-as-fleets” approach (Waterhouse et al. 2014) when the first integrated model was used to assess the stock (A-SCALA, Maunder and Watters 2003). In 2009, the assessment model ([Maunder and Silva, 2010](#)) was migrated to the Stock Synthesis platform (Methot and Wetzel 2013), with similar assumptions to those in the A-SCALA models. The integrated models used indices of abundances derived from both the longline and the purse-seine fisheries, while relying heavily on the information from the length composition data as well as catch data (e.g., [Minte-Vera et al 2021](#)). However, the longline and the purse-seine indices showed discrepancies that could not be explained by addressing potential changes in target for the longline fleet, misspecification of growth, or inadequate consideration of spatial structure in the indices of abundance ([SAC-10-Inf-F](#)). The 2019 assessment was considered not reliable by the IATTC scientific staff to produce management advice due to the high influence of the longline index, which may be related to a different stock or sub-stock than the one exploited by the main purse-seine fishery that associated with dolphins.

We attempted to explore the spatial structure of yellowfin tuna in the EPO for the 2019 external review ([YFT-02](#)), but no clear stock definition was available. The review panel recommendations were:

- Data and models should be consistent with explicit and plausible hypotheses and conceptual models. For example, if a model is nominally a spatial model, the spatial domain should be defined, and the data preparation and model should be consistent for the spatial domain.
- Given the information supporting the two-stock hypothesis was suggestive rather than conclusive, alternative models should continue to be developed that are consistent with both one-stock and two-stock hypotheses as well as models somewhere in between those extremes.
- If models with alternative stock structure are developed, management consequences of using a two-stock hypothesis if a one-stock hypothesis was true (and vice versa), should be evaluated (e.g., Risk Analysis)

For the 2020 benchmark assessment, the following the recommendations of the review panel, we developed a conceptual model for yellowfin tuna to address the key uncertainties in the stock and to guide the development of the assessment model and associated risk analysis. The spatial structure was recognized as the main uncertainties for yellowfin tuna.

Because of the strong evidence of spatial structure of yellowfin in the EPO and the uncertainty about the boundaries and mixing between those putative stocks, three overarching hypotheses about the degree of mixing between stocks within the EPO were proposed and the inconsistencies between the various indices were addressed (Figure 1). The three overarching hypotheses were “High mixing”, “Episodic/high-variability mixing”, and “Negligible mixing”. The High mixing hypothesis is represented by single-stock models like previous assessments. The Episodic/high-variability mixing hypothesis is represented by single-stock models that are driven by either the northern or the southern stock data. This means that each model should be fit to the data for the north (or south) and only uses the catch for the south (or north) while fixing the selectivity for these fisheries. The Negligible mixing hypothesis is represented by two independent assessments, one for the north and one for the south. The uncertainty on how to divide the catches between a “north” and a “south” stock implied that only the High mixing hypothesis was practical to implement at that time. The episodic mixing and the negligible mixing hypotheses lacked a refinement on how the stock should be split, which is needed so that those hypotheses can be modelled using integrated models.

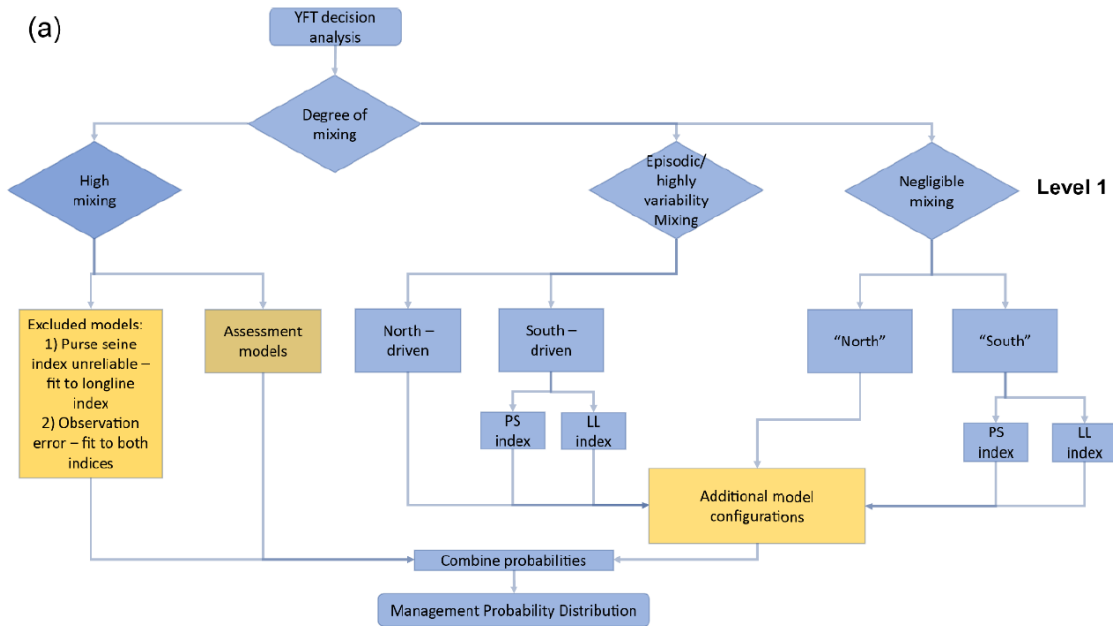


FIGURE 1. Conceptual model for yellowfin in the EPO depicted as flow charts identifying the set of overarching hypotheses. Only the high mixing hypothesis was translated into population dynamics models in the 2020 assessment and risk analysis (From: [SAC-10-INF-J](#))

UPDATE OF THE CONCEPTUAL MODEL FOR YELLOWFIN TUNA IN THE EPO

A thorough literature search was done and the conceptual model for the dynamics of yellowfin tuna in the EPO was updated. Conceptual models are simplified representation of the understanding and uncertainties about the main components of a system and their relationships (Minte-Vera et al in prep). Conceptual models are then used as the basis for the assessment models, as the analysts translate the concepts into the assessment model components.

The updated conceptual model for yellowfin tuna in the EPO considers the indication that there is spatial structure and the latest scientific information regarding the stock. The reviewed information points to at least two genetically different populations of yellowfin tuna present in the EPO (**Figure 2**). The boundary between the populations is dynamic as the populations are associated with distinct marine biogeochemical provinces which change dynamically, expanding the favorable habitat for one population while contracting the favorable habitat for the other population and vice-versa, in response to oceanographical variation.

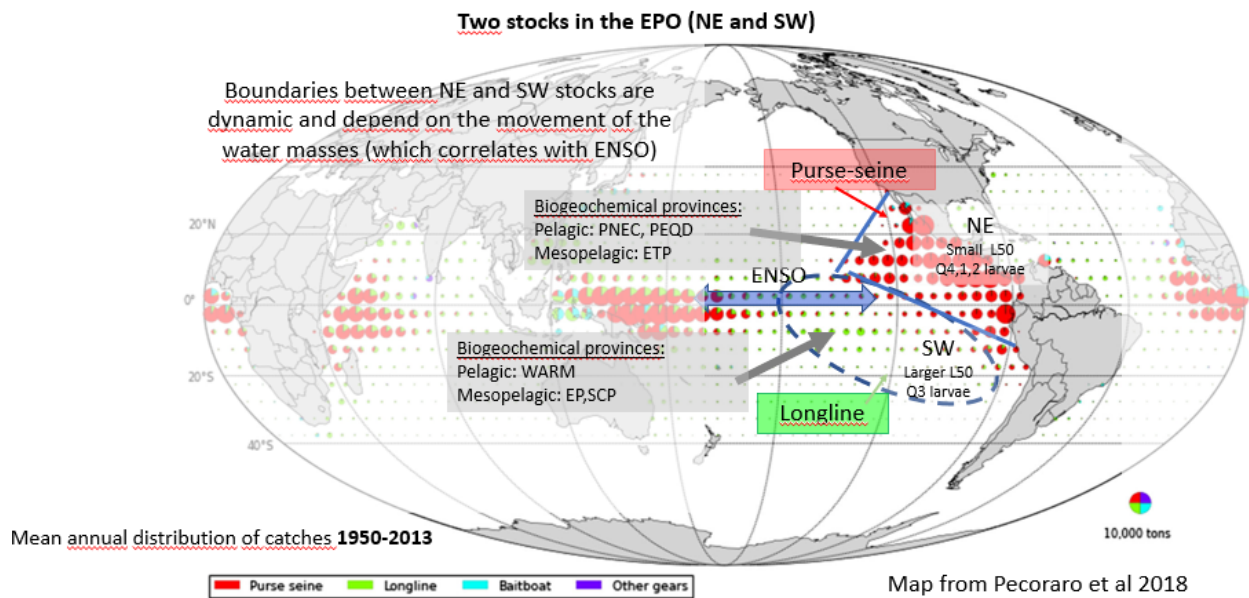


FIGURE 2. Updated conceptual model for yellowfin tuna in the EPO. There are two stocks in the EPO (NE and SW), roughly corresponding to the current area of operation of the purse-seine sets on dolphins' fleets (NE), current area of operation of the longline fleet (SW). The stocks occupy the Longhurst epipelagic biogeochemical provinces: NE stock: North Pacific equatorial counter current (PNEC), Pacific equatorial divergence (PEQD), SW stock: Western Pacific warm pool (WARM), South Pacific gyre (SPSG). The stocks occupy the mesopelagic biogeochemical provinces: NE stock: Eastern Tropical Pacific (ETP) and SW stock: Southern Central Pacific (SCP) and Equatorial Pacific (EP)

Molecular studies

Genetic, genomic, and other molecular studies point to a separation in at least two populations in the EPO (**Figure 3**, Ward et al 1994, Ward et al 1997, Díaz-Jaimes and Uribe-Alcocer 2006, Grew et al 2015, Pecoraro et al 2015, Muñoz-Abril et al 2022). One population would be distributed closer to the coast of the Americas and the other closer to equatorial waters along the 150°W IATTC boundary line, which will encompass the CPO and may even extend to areas off Perú in some years. The allelic frequency of the GPI-A* gene was similar in the samples taken closer to the coast of the Americas and different from the samples taken in WCPO, including Hawaii (Ward et al 1997). No genomic differentiation was found between fish from the coast of Ecuador and northern Perú (landed at Santa Rosa port in Ecuador), Galapagos Islands (Ecuador), and Cabo San Lucas (Mexico) (Muñoz-Abril et al 2022), but genomic differences were found between fish sampled in Baja California and Tokelau (Grewe et al 2015). Those two samples were different from those in the Coral Sea, which may indicate yet another population (Grewe et al 2015). Differences in microsatellite variation were found between fish sampled off Perú and fish sampled in the northern hemisphere (Gulf of California, SW Revillagigedo Islands, and near Clipperton Islands) (Díaz-Jaimes and Uribe-Alcocer, 2006). Fish caught around Hawaii (of 30-60 cm or 0.5 to 1 years of age) have similar concentrations of stable isotopes and trace elements at the otolith's core, and different from other areas, which may be an indication of similar origin (Wells et al 2012, Rooker et al 2016). Similar chemical analyses indicate that fish caught in western equatorial areas of the western Pacific Ocean (WPO) do not share the same elemental concentration in their otolith core with fish caught in the CPO, which may indicate they originated from different locations (Rooker et al 2016). Using close

kin analyses, a high proportion of half-sibling and sibling pairs were identified from fish sampled in the exclusive economic zone of the Federate Sates of Micronesia (Anderson et al 2019), which may indicate yellowfin from those discrete equatorial areas of the western Pacific Ocean (WPO) may be from a resident stock.

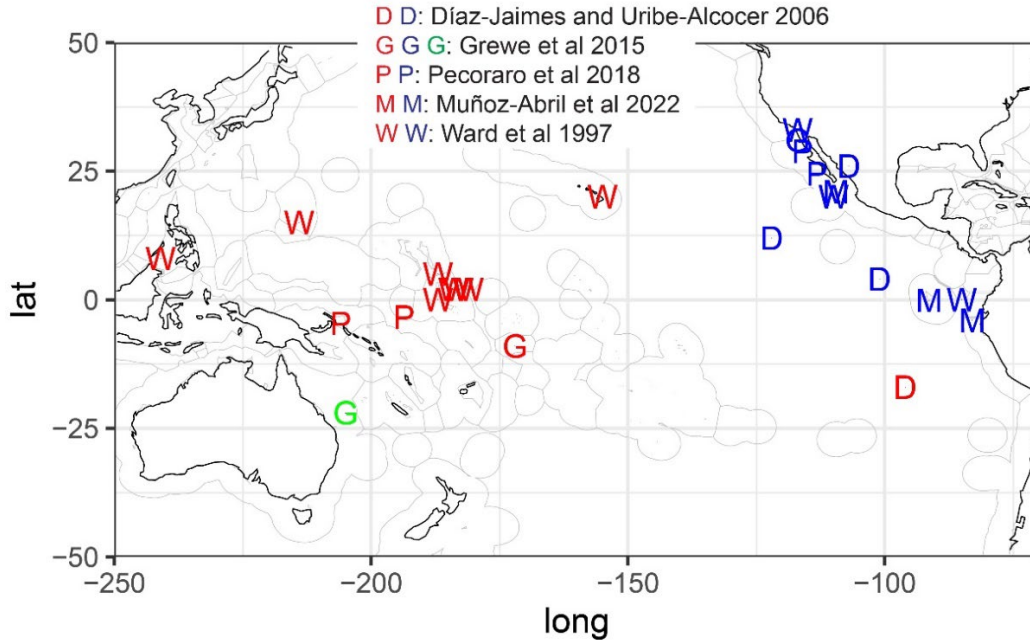


FIGURE 3. Genetic and genomic studies of yellowfin tuna in the Pacific Ocean. The letters indicated the study. Different color within each study indicates that fish sampled in these locations are genetically or genomically different, while same color indicate similarity. There may be several stocks of yellowfin tuna across the Pacific Ocean and two 2 different stock in the EPO.

Larval distribution and reproductive biology

In the EPO, spatial differences in larval distribution and reproductive biology are present.

The two presumed populations in the EPO have higher larval abundance in different times of the year (**Figure 4**). In the waters close to the coast of the Americas, the highest larval abundance is in quarter 1 and 2 and to some extent in quarter 4 (Suzuki et al 1978). In the CPO the largest larval abundance is found in quarter 3. Suzuki et al (1978) combined the larval abundance samples (surface horizontal tows) taken by Japan’s Far Seas Fisheries Research Laboratory, from 1956-1971, with the IATTC data for the EPO (Klawe 1963). From those samples, Suzuki et al (1978) identified three areas with high density of larvae in the Pacific Ocean: eastern area (east of 110°W), central area (130°W – 160°W) and western area (130°E-170°E)

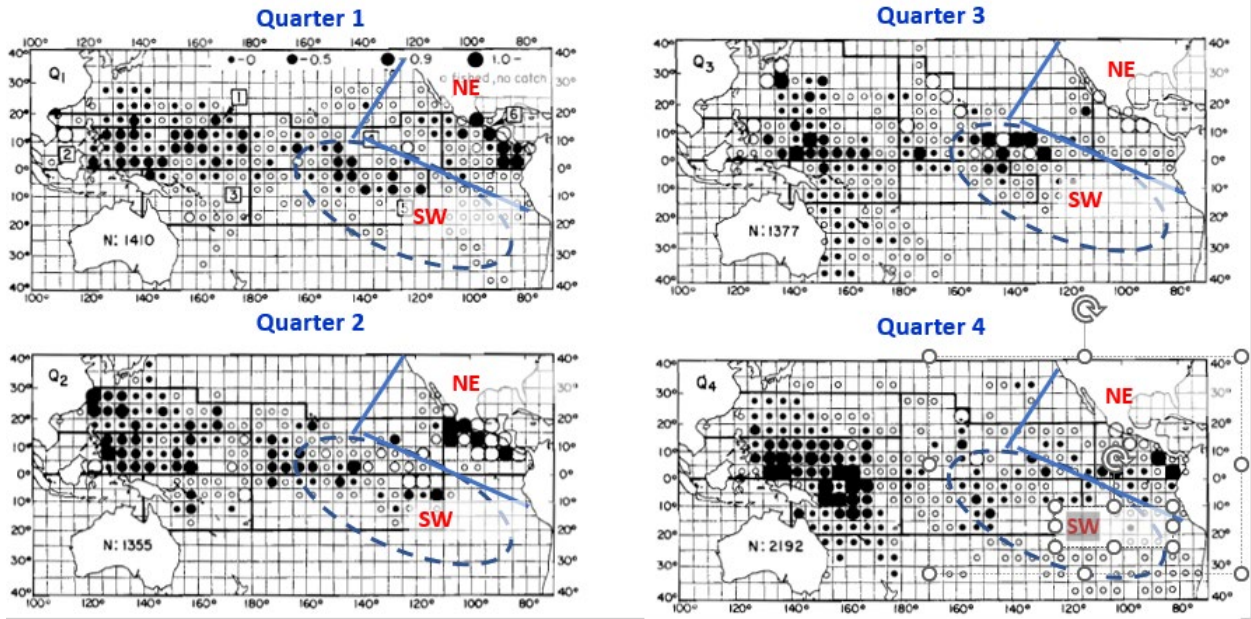


FIGURE 4. Yellowfin larval distribution by quarter with the hypothesis of two yellowfin tuna stocks in the EPO, a northeast stock (NE) and a southwest stock (SW). The larvae data abundance comes from a compilation of samples (surface horizontal tows) taken by Japan’s Far Seas Fisheries Research Laboratory (1956-1971) and IATTC data for the EPO (Klawe 1963). From Suzuki et al (1978).

Reproductive biology studies show spatial variability in length at 50% maturity for both males and females (Schaefer 1998, **Figure 5**). Yellowfin sampled closer to the coast have larger size at 50% than those sampled closer to the CPO, at least for data collected between 1987-1989 (**Figure 5**). A new reproductive biology study (Schaefer and Fuller 2022) for female yellowfin tuna in the EPO did not collect data in the same locations, but in four distinct areas (**Figure 6**). Females sampled south of 5°S showed different patterns than those sampled north of that latitude. According to the updated CM for yellowfin tuna in the EPO, the areas south of 5°S may have fish from the SW and the NE stock, in different years or seasons. According to the updated conceptual model, the SW stock would not have much reproductive activity in the areas sampled by Schaefer and Fuller (2022).

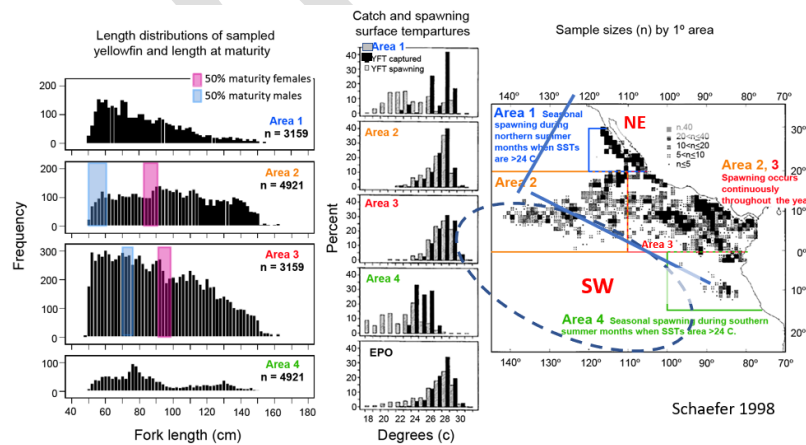


FIGURE 5. Summary of the reproductive biology study by Schaefer (1998) indicating the at 50% maturity for males and females of yellowfin tuna in different areas of the EPO.

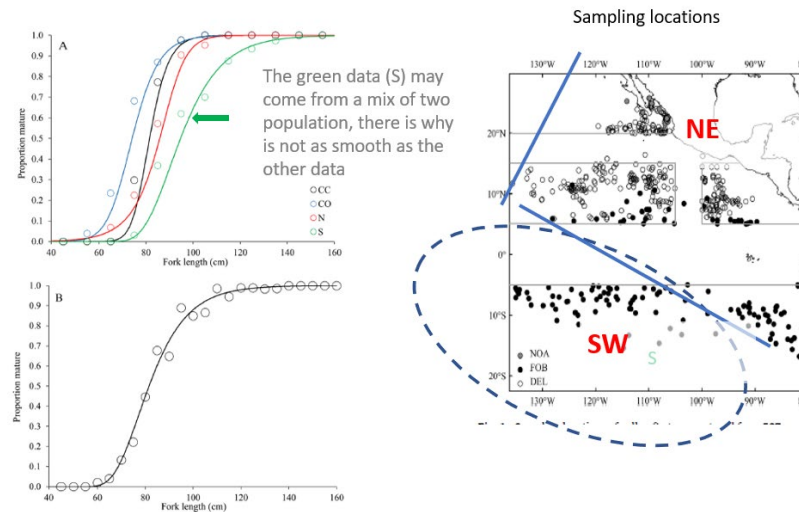


FIGURE 6. Summary of the reproductive biology study by Schaefer and Fuller (2022) indicating the size at 50% maturity for females in several areas of the EPO.

Dynamic boundaries and mixing

We hypothesize that the boundary between the two populations is dynamic. The distribution of the two populations would cover roughly three mesopelagic and three epipelagic biogeochemical regions (Sutton et al 2017, Longhurst 2007, Reygondeau et al 2013). The mesopelagic regions (**Figure 7**) are Eastern Tropical Pacific (ETP), the Equatorial Pacific (EP), and South-Central Pacific (SCP) as defined by Sutton et al (2017)¹. The ETP is characterized by high productivity, extensive layering of water masses, a shallow and abrupt thermocline, and very low oxygen at mesopelagic depth (Fiedler and Talley, 2006). These conditions may promote the peculiar association between dolphins, mainly spotted dolphins (Scott et al 2012) and adult yellowfin tuna, which is why purse-seine fishers set around dolphin herds to catch yellowfin tuna. The EP is characterized by a complex combination of eastward and westward currents and almost permanent semi-pelagic upwelling, while the SCP is associated with the oligotrophic southern Pacific Gyre system (an area of spillover of yellowfin mostly originated in the EP in our model). The epipelagic regions are North Pacific equatorial counter current (PNEC) and Pacific equatorial divergence (PEQD) (Longhurst 2007, Reygondeau et al 2013), which roughly sit on top of the ETP and the western Pacific warm pool (WARM), which roughly sits on top of the EP (**Figure 8**). The two populations in the EPO would be associated with the ETP (PNEC+PEQD) in the east and the EP (WARM) in the west and could be indexed by the dolphin-associated purse-seine index and longline index, respectively (**Figures 7 and 8**).

¹ defined biogeographical mesopelagic regions based on distributional patterns of pelagic fauna or regions particularly characterized by environmental factors acting as key ecological drivers.

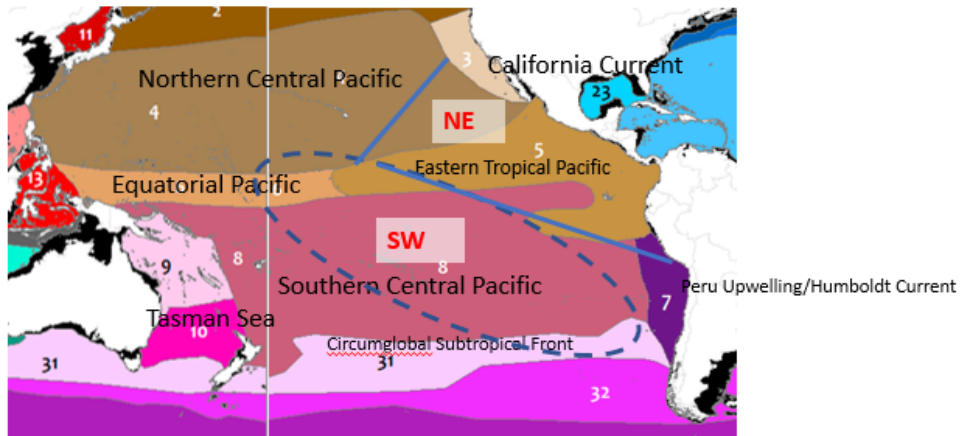


FIGURE 7. Mesopelagic regions of the Pacific Ocean (edited from Sutton et al 2017)

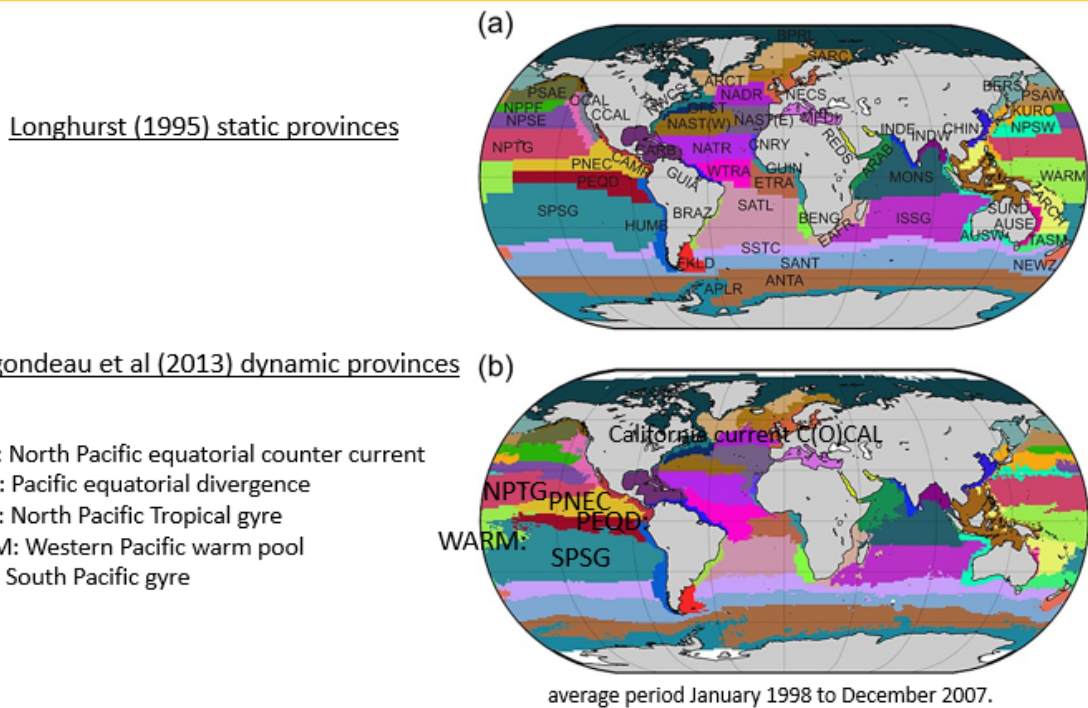


FIGURE 8. Epipelagic regions of the world (From Reygondeau et al 2013)

The size of the area occupied by the biogeochemical regions changes with variation in oceanographic conditions (Oliver and Irwin, 2008, Reygondeau et al, 2013). The ETP area compresses in El Niño, while the EP/WARM area expands; the opposite is true in La Niña (**Figure 9**). The tropical tunas can reproduce when the sea surface temperature is greater than 24°C (Schaefer 1998), and recruitment is hypothesized to be related to the area of favorable habitat (Maunder and Deriso 2013). The two populations would have conditions for expansion in either La Niña (Northeast population associated with ETP) or El Niño (Southwest population associated with the EP/WARM).

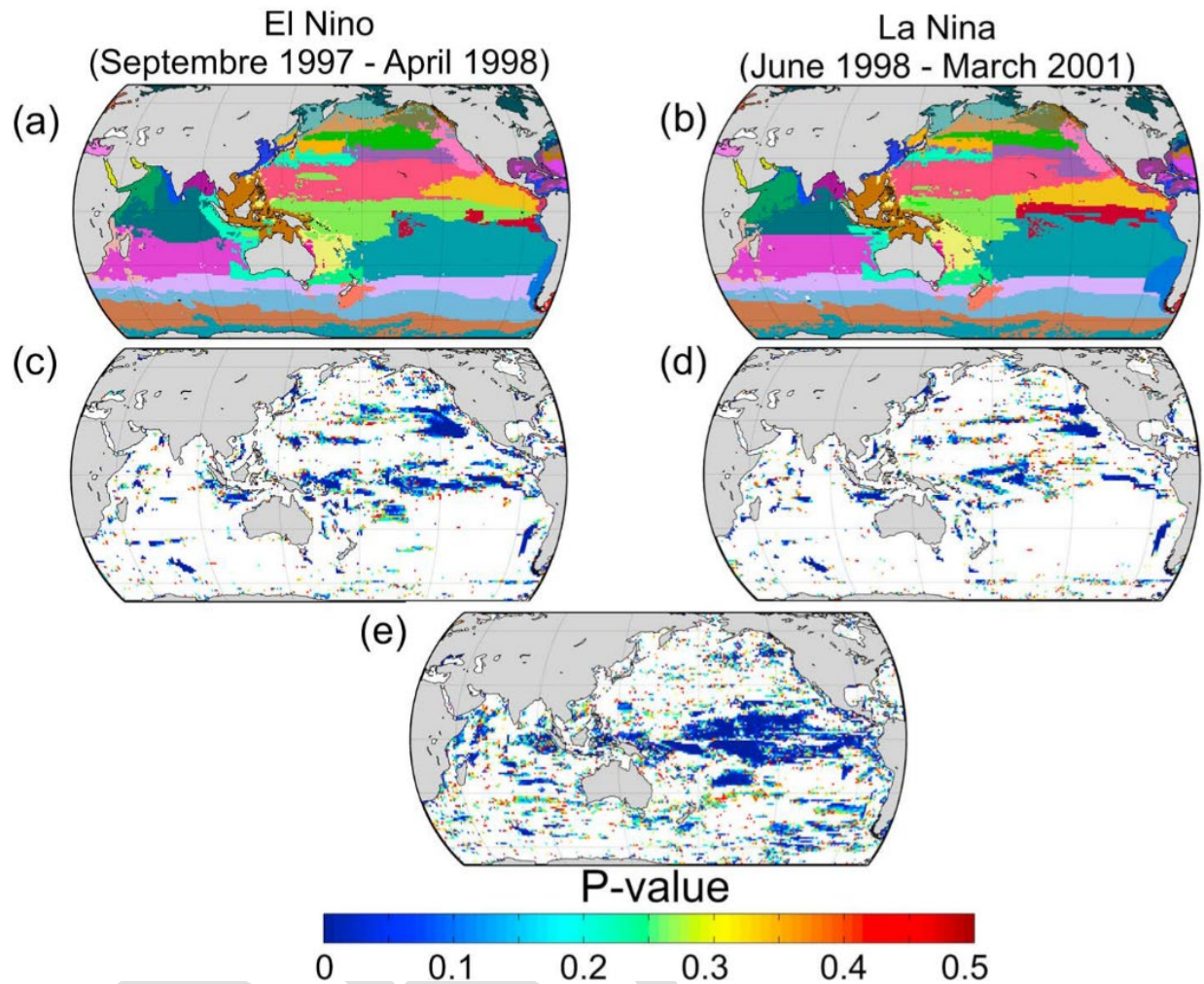


FIGURE 9. Dynamic changes of the epipelagic regions of the world (From Reygondeau et al 2013). (a) Biogeography of the global ocean for the 1997/1998 El Niño event (September 1997 to April 1998). (b) Biogeography of the global ocean for 1998/2001 La Niña event (July 1998 to March 2001). (c) Map of the significant change (p value ≤ 0.05) in the probability of occurrence between El Niño months and normal conditions. (d) Map of the significant change (p value ≤ 0.05) in the probability of occurrence between La Niña months and normal conditions. (e) Map of the significant change (p -value ≤ 0.05) in the probability of occurrence between El Niño months and La Niña months. The extratropical Northern Oscillation Index was used to detect the El Niño, La Niña, and normal conditions.

Tagging data

The tagging data is compatible with the conceptual model proposed here (**Figures 10a, 10b, 10c**). The fish tagged in the EPO with archival tags, close the coast of the Americas, tend to stay in those areas. The fish tagged in the CPO tend to either stay in the tagged area (Schaeffer and Fuller 2021) or move to the east or west (SPC unpublished tagging data, **Figure 10c**). The earlier tagging data in the EPO suggest at least that the fish stayed closer to the tagged areas (**Figure 10b**); however, this needs to be interpreted

considering historical fishing effort². It is plausible that movement may be tied to the position of the water masses from the different biogeochemical provinces (Figure 9).

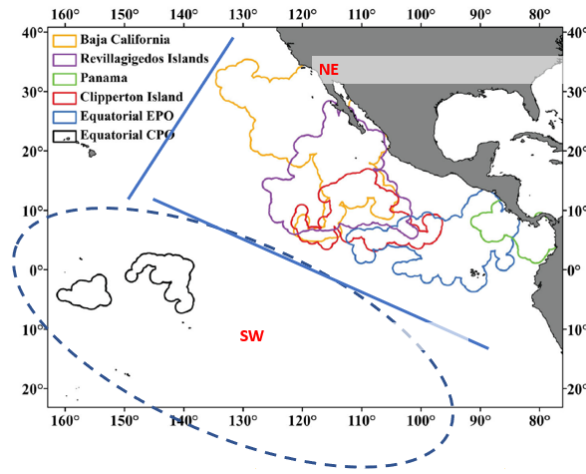


FIGURE 10a. IATTC archival tagging data: 100% volume contours (utilization distribution) for yellowfin tuna in the EPO. The hypothetical distribution of the NE and SW yellowfin tuna stocks in the EPO is overlaid. From Schaefer and Fuller (2021).

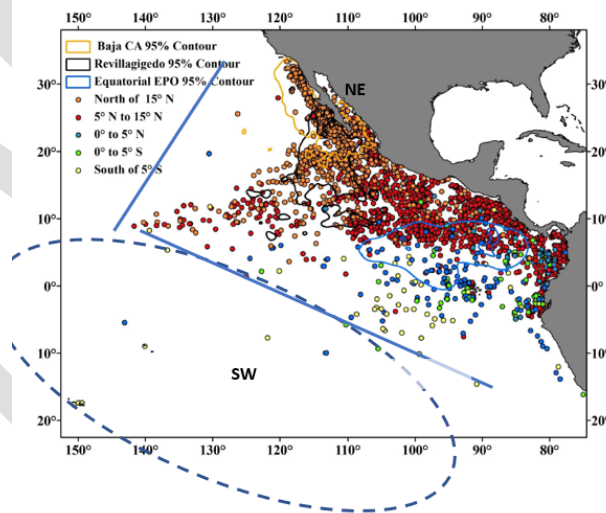


FIGURE 10b. IATTC conventional tagging data³: recovery location color coded by release region, and 95% contour (utilization distribution) for fish tagged with archival tags in three regions. The hypothetical distribution of the NE and SW yellowfin tuna stocks in the EPO is overlaid.

² Much of the tagging data is coastal, so it could be somewhat misleading and that should be taken into consideration when interpreting the tagging data. Yellowfin tuna seems to move in all directions, but movement is somewhat restricted. Any apparent stock structure boundaries from the tagging data need to be interpreted in terms of the recapture effort. First, the fishery did not move offshore until 1969 and did not catch much yellowfin south of 5°S before 1976 (Watters 1999). Note that not much tagging was done around the equator after 1975. Second, the CYRA had boundary at 115 and 120 (depending on the year) between 5°N and 20°N. The area between 115-120°W was open during 1976-1979.

³ The maps are produced from speed filtered conventional tag data for two separate time periods, 1960 – 1981 (n=11,371) and 2000 – 2015 (n=1,589). The data is filtered for unrealistic speeds. The speed filter is derived from both archival tag and high

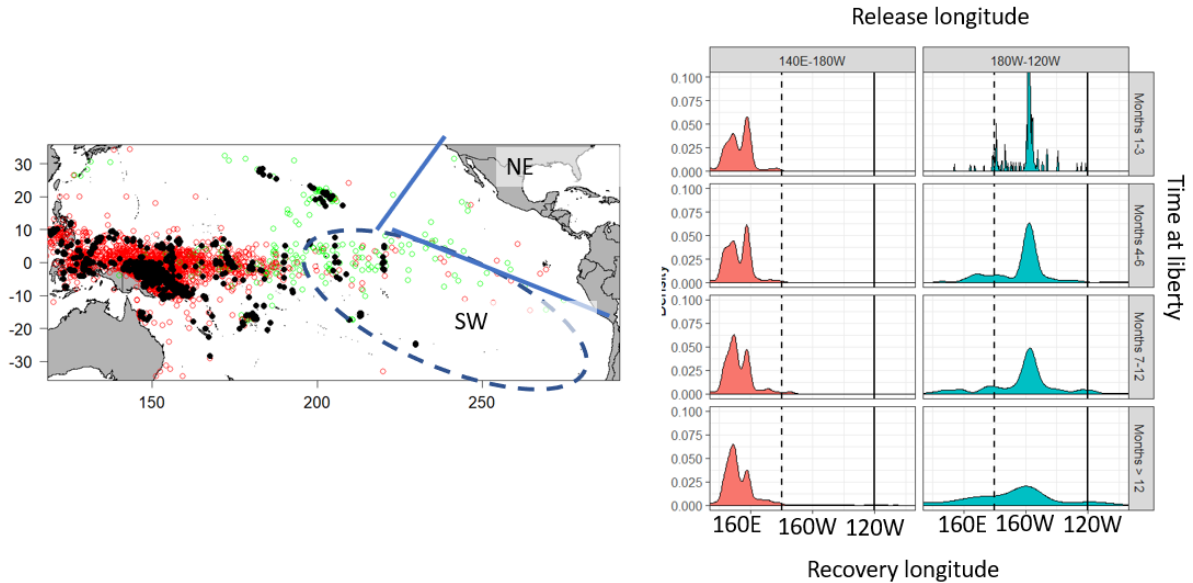


FIGURE 10c. Western and central Pacific Ocean tagging data. The hypothetical distribution of the NE and SW yellowfin tuna stocks in the EPO is overlaid. The data includes all tags that have a release and recapture locations, and a date at recapture greater than 30 days in The Pacific Community (SPC) database (November 2019). The release locations are black dot. Recovery data are color coded by release region: red dots are fish released west of 180°W and the green dots were released between 180°W and 120°W. Some tags in this plot that may not be included in the WCPO yellowfin tuna stock assessment, because they are from a program that are not used or lack a recapture gear, or other information. There is not much auxiliary information apart from the recovery location of the tags recovered in the EPO. Elaborated by Mathew Vincent (SPC) by request from the authors.

DYNAMIC DISCRIMINATION OF STOCKS

Principal component analysis on oceanographic variables

To investigate the possible discrimination of the two stocks by the biogeochemical provinces they inhabit, oceanographic variables that may characterize the provinces were summarized using a Principal Component Analysis (PCA, Appendix A).

The first two principal components explained 80% of the variability: 66% by the first principal component (PC1) and 14% by the second (PC2). PC1 was strongly negatively correlated with mixed layer depth (MLD), the isothermal layer depth (ILD, which is an index of the depth of the surface mixing), salinity (SAL), and temperature at 100 meter (m) depth (SST_100). PCA2 is highly positively correlated with SST (Figure A2).

confidence conventional tag data and considers both speed and days at liberty. Fish which are at liberty for shorter periods of time can move at greater speeds (26.1 nm/day) than those at liberty for extended periods (11.7 nm/day). Even with the speed filter applied, inaccurate recovery information may still be present. The 95% contours for archival tags released along Baja California (tags = 126, positions = 31,549), at the Revillagigedo Islands (tags = 45, positions = 14,321), and in the equatorial EPO (tags = 5, positions = 476) are also added. Exact release locations are not included; however, recoveries are color coded by release region. Five release regions were mapped: North of 15° N (n = 9,368), Between 5° N and 15° N (n = 2,657), 5° N to 0° (n = 673), 0° to 5° S (n = 206), and South of 5° S (n = 56).

The maps of PC1 show a gradient from the northeast to the southwest of the EPO (Figure 11), while the PC2 shows the separation of the area of influence of the California and Humboldt current in the north and the south, respectively.

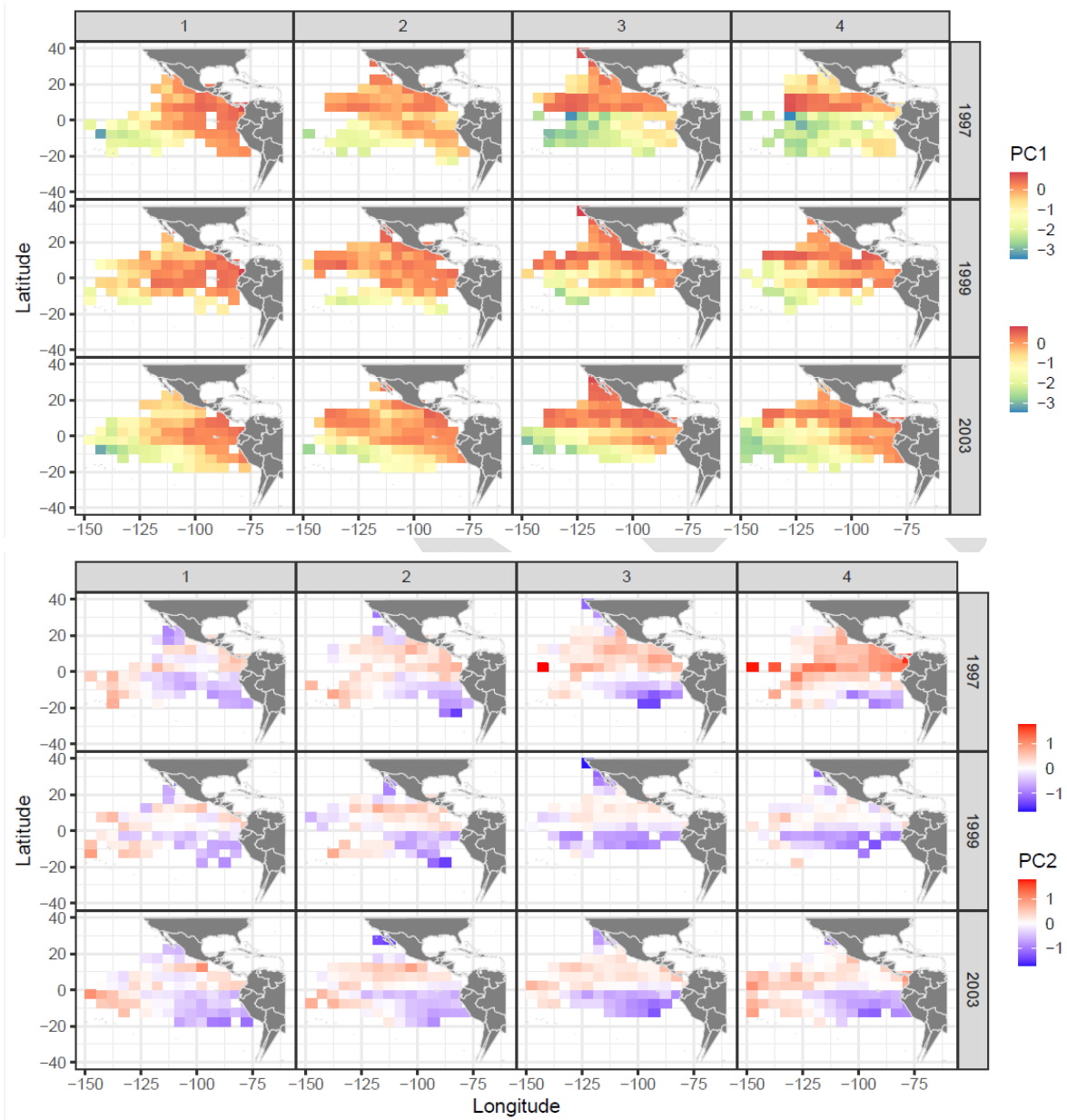


FIGURE 11. Examples of maps of the principal components 1 (PC1, 66% variance explained) and 2 (PC2, 14%) on oceanographic variables by quarter and year (1997 – El Niño, 1999 – La Niña, 2003 – Neutral). When PC1 increases, the following variables decrease: mixed layer depth (MLD), the isothermal layer depth (ILD), salinity (SAL), and temperature at 100 m depth (SST_100). When PC2 increases, SST increases. When PC2 increases, sea surface temperature increases (SST).

Tree analysis of length composition data

The length frequency data (**Appendix B**) for yellowfin tuna from the purse-seine fleet fishing on floating objects was analyzed to investigate whether it would support a separation along the environmental axes

as summarized by the PCA. We focused on floating object sets (but see SAC-14-INF- for the analysis on data from dolphin sets and unassociated sets), as they catch a greater proportion of smaller tuna that may be, in principle, more likely to be caught closer to the area from which they originated than larger fish. Additionally, it gives some indication of the pattern shown by fish that may not yet have the full capacity for endothermy developed, and maybe foraging in shallower waters than larger fish. “ Once yellowfin can regulate their internal temperature, they can explore deeper waters such as the top of the mesopelagic region (Bernal et al 2017), thus its distribution may change to more suitable deeper habitats. It is estimated that the minimum length for a yellowfin to maintain the temperature of its muscles 3°C above the water temperature is 35 cm fork length (Dickson and Dickson 2019). This size corresponds about 2 quarters of age (Wild 1986). Fish larger than 35 cm will expand their thermal niche and explore deep and colder waters as they grow.

A tree analysis using length frequency data (**Appendix B**) was used following the methods by Lennert-Cody et al (2010, 2013) with a slight modification. The spatial predictors (latitude and longitude) used by Lennert-Cody et al (2013), were not used. Instead, the first two principal components were used as “spatial” predictors (**Appendix B**). The temporal predictors used were quarter (1- January to March, 2 – April to June, 3 – July to September, 4 – October) or cyclic quarter (when quarter 4 is similar to quarter 1). The chosen number of splits for each tree was 3.

The tree analysis that explained the most variability of the length frequencies of the floating objects sets is one has the first split on PC2 = -0.25 (**Figure 12**), which separates colder areas from the tropical areas. These are areas that roughly correspond to the influence of the Humboldt current in the south (and California current in the north), from the central warm area (**Figure 13**). Alternative first splits that have high support are quarters and PC1 at about -1.00 (**Figure 12**). The second and third splits of this tree, split the colder area in quarters (2nd split: separate quarters 4 and 1 from 2 and 3, 3rd split: separate quarters 1 and 4) highlighting the seasonal effect in those areas, as expected (**Figure 14**). For second split, there was also an increasing support for a split on PCA1 at around -1.00 for both colder and warmer areas (**Figure 15**).

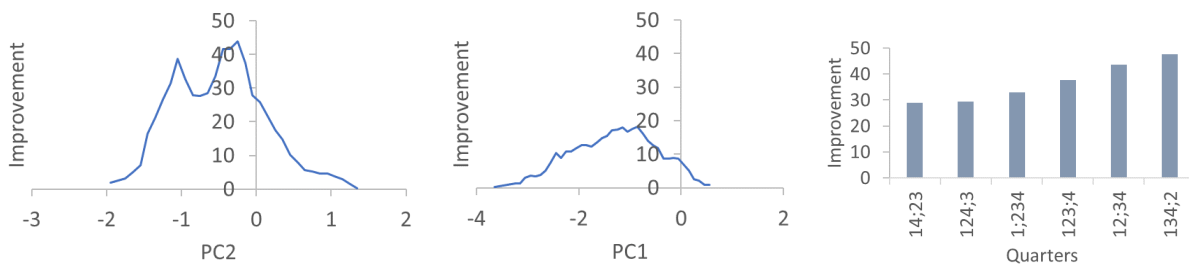


FIGURE 12. Improvement related to the different options for first split.

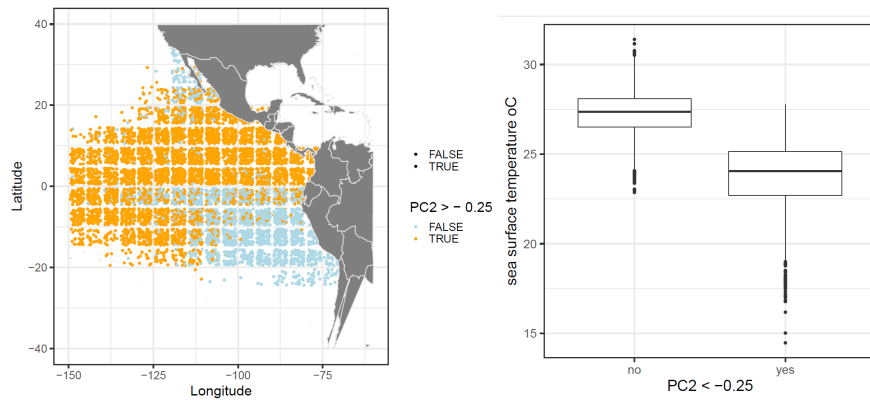


FIGURE 13. All areas in the EPO with $PCA2 < -0.25$ and boxplot of the sea surface temperature associated with those areas.

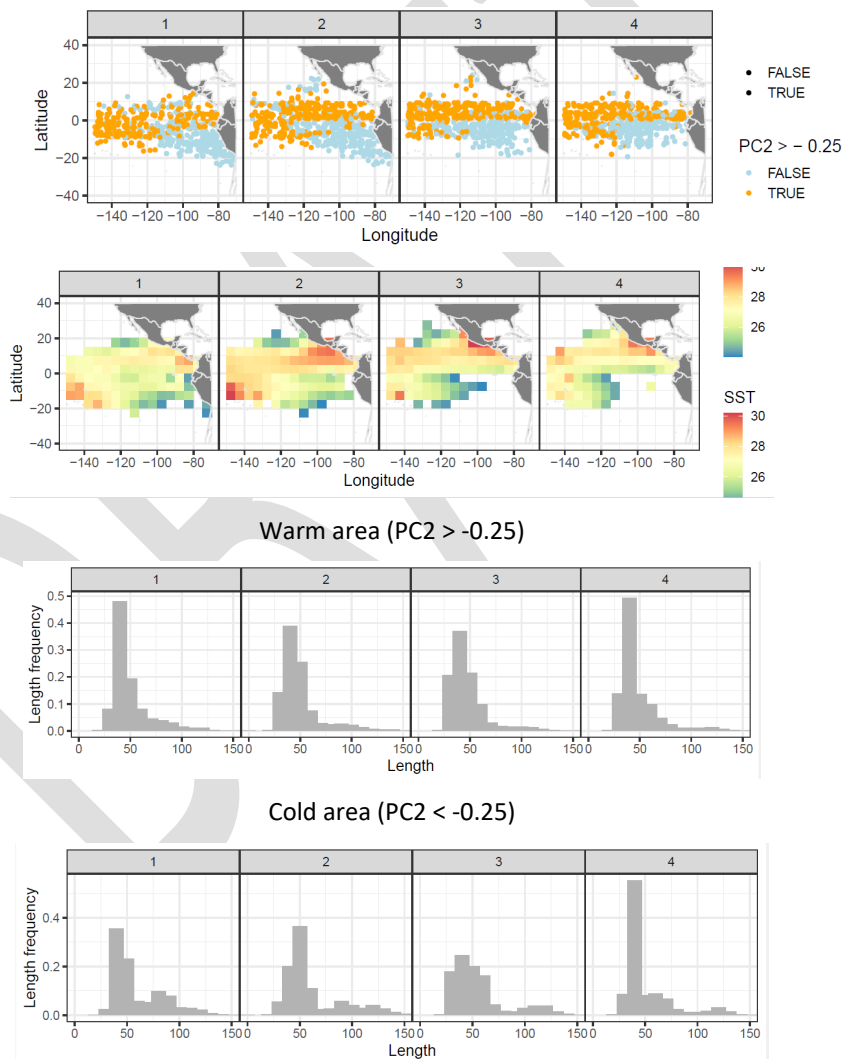


FIGURE 14. Position of the OBJ sets for areas corresponding to the first split of the tree analysis using length frequency data from the port sampling for each quarter (1995-2017 combined). Middle panel: SST above 24°C (medians over 1995-2017 in each 5° x 5° cell). Bottom panel: mean length frequencies for the warmer area ($PCA2 > -0.25$) and colder area ($PCA2 < -0.25$).

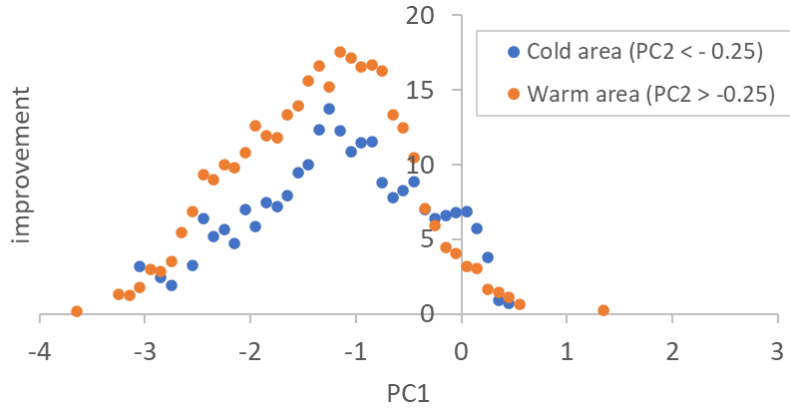


FIGURE 15. Support for the second splits for areas 1 and 2 along the PC1 axis.

A new tree analysis was run removing the colder areas (data with PCA2 < -0.25). This new tree analysis clearly showed the split at PCA1 < -1.15 (**Figure 16**, Table 1), which split the gradient in a northeast to southwest direction (**Figure 17**). The second and third split of this tree separated quarters 1 and 2 from 3 and 4 in the east and the west area, respectively, indicating the effect of growth over the quarters.

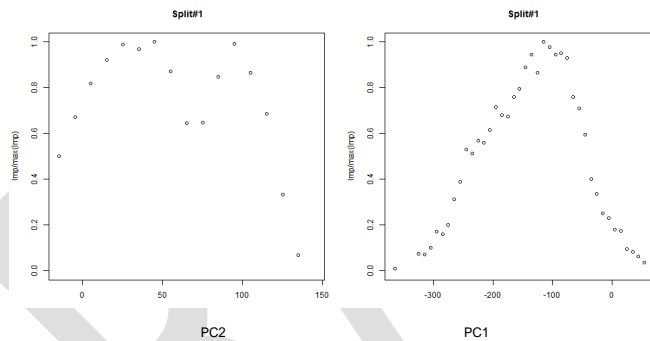


FIGURE 16. Support for splits along the two environmental gradients summarized the two principal components.

Table 1. Improvement

Explanatory variable	Value	Improvement
PC1	-1.15	17.54719
Cyclic quarte	134;2	17.19459
PC1	-1.05	17.12858
PC1	-0.85	16.68399

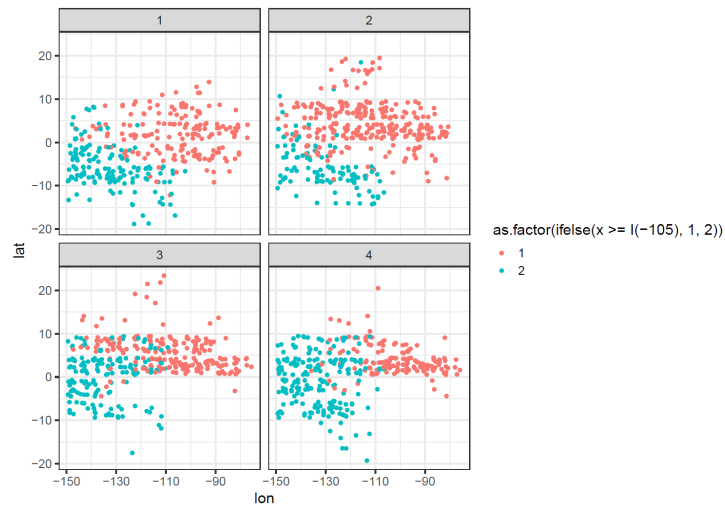


FIGURE 17. Position of the OBJ sets in warmer areas corresponding to the first split of the tree analysis using length frequency data from the port sampling.

The split at -115 along the east-west gradient was considered as a potential candidate to split the putative two stocks.

The areas defined by the splits along PC2 and, for the warmer area, along PC1 are shown in **Figure 18**. The NE area, the ST_100 is around 14°C, the MLD, and the ILD are shallower, while in the SW area the ST_100 is about 23°C, the MLD, and ILD are deeper (**Figure 18**). According to the water column structure, the colder area is more like the northwestern area, as it shows similar SST_100, MLD, and IDL.

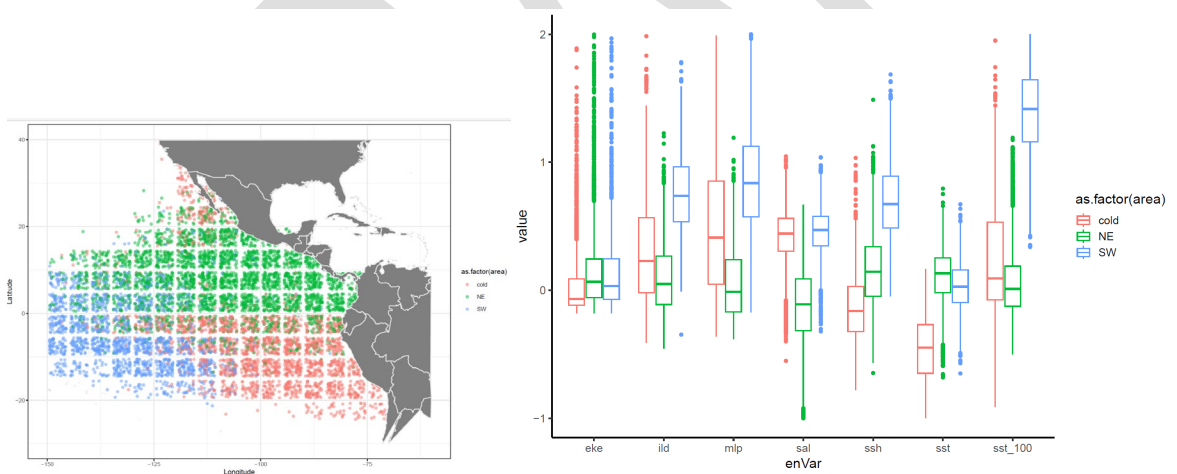
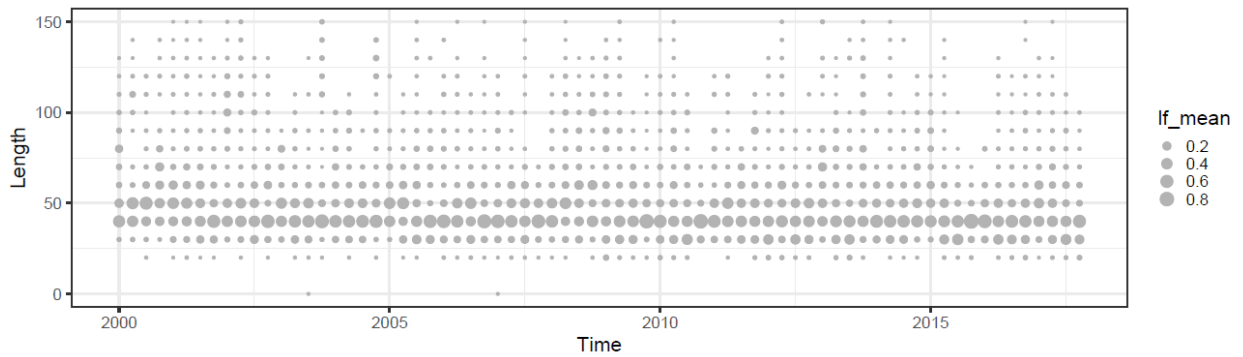


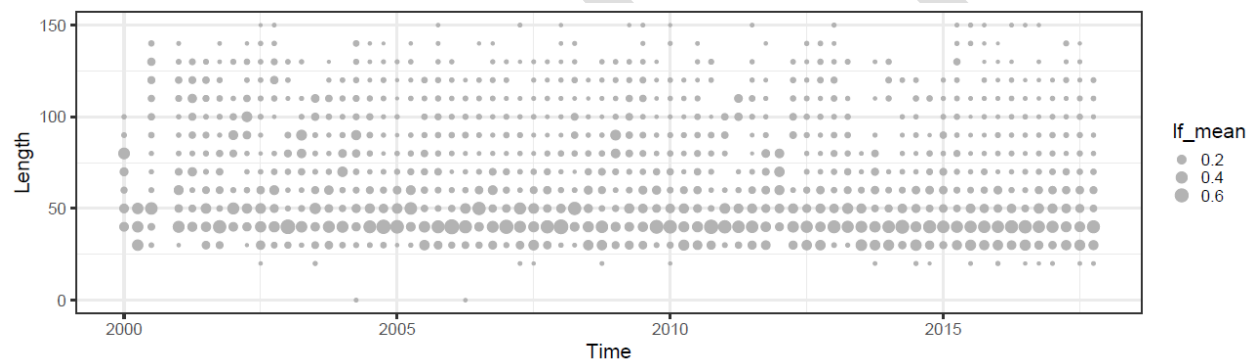
FIGURE 18. (Right panel) Position of all purse-seine sets in the areas resulting from split along the environmental gradients guided by the length composition data of the floating object fishery. The cold areas ($PC2 < -0.25$), warm area closer to the coast ($PC2 > -0.25$ and $PC1 > -1.15$) and warm area offshore ($PC2 > -0.25$ and $PC1 < -1.15$). (Left panel) Boxplot of the (normalized) environmental variables for those areas.

The length compositions for the floating objects for the three areas as in **Figure 19**.

Tropical coastal (PC2 > -0.25 and PC1 > -1.15)



Tropical offshore (PC2 > -0.25 and PC1 < -1.15)



Humboldt current area (PC2 < -0.25 and latitude < 0)

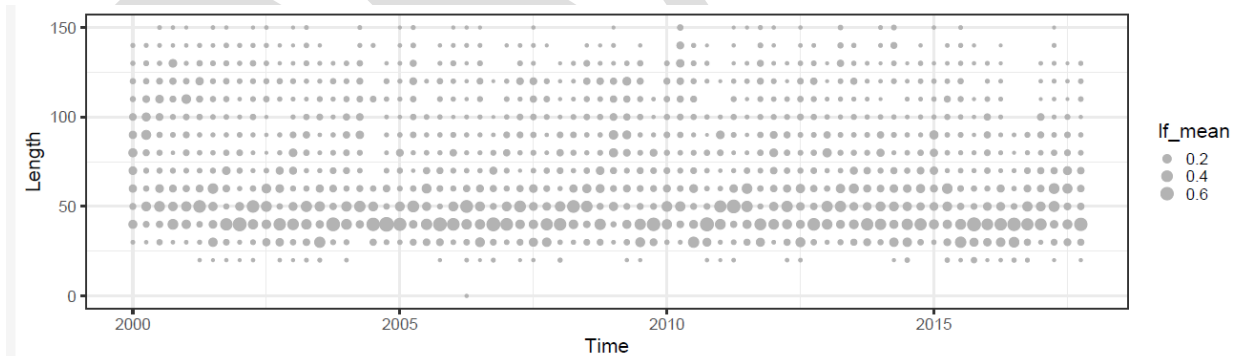


FIGURE 19. Length frequencies raised to the well totals obtained in the port sampling program for the purse-seine on floating object fisheries from 2000-2017, by quarter for the three areas defined .

Stock separation

The split at $PCA1 \leq -1.15$ was used to discriminate between the preferential habitats for the two stocks. The colder area was split along the PC1 as well to allocate the sets in that area to either the NE or SW areas. When the two areas defined by this split are mapped (using the data for all purse-seine sets), it is possible to depict the dynamic nature of their boundaries (**Figure 20**). In El Niño years, the SW area moves closer to the coast, while in La Niña conditions, the NE area moves towards the west as expected if the selected variables were correctly indicating the two main dominant water masses (**Figure 20**).

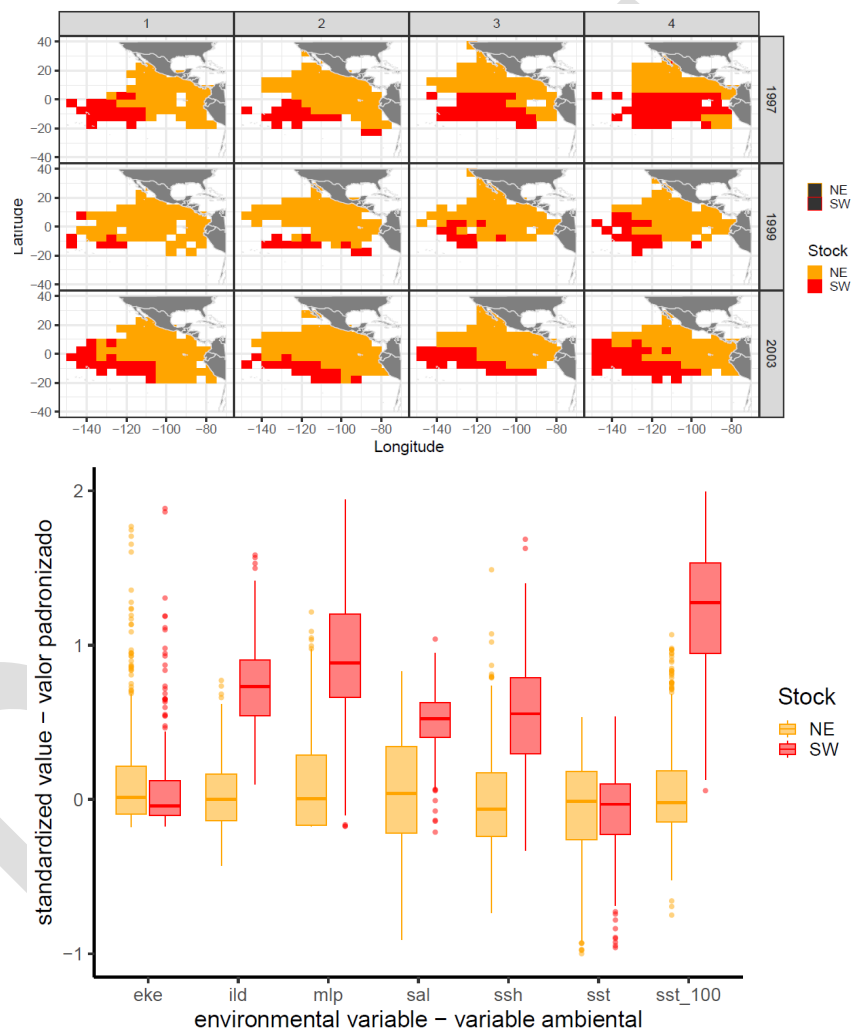


FIGURE 20. Top: classification of 5 by 5 cells in the northeast (NE) and southwest (SW) putative stock, by quarter and year (1997 – El Niño, 1999 – La Niña, 2003 – Neutral). The areas as classified using a split along the PC1 environmental gradients, which summarized the water column structure, guided by the length composition data of the floating object fishery. Bottom: boxplot of medians of oceanographic variables by stock (standardized).

When the purse-seine catches from sets on dolphins are mapped, they lay almost invariably in the NE area (**Figure 21**), as expected, given the conceptual model for the stock. Yellowfin caught in unassociated and floating object sets are distributed within both areas (**Figures 22, 23**), with slight predominance of

unassociated catches in the NE area. The longline catches are distributed in both provinces, but larger catches are seeing in the SW area (**Figure 24**). The catches for longline fisheries not allocated to the two areas will be allocated to the SW area in the southern hemisphere and to the area “north” in the northern hemisphere.

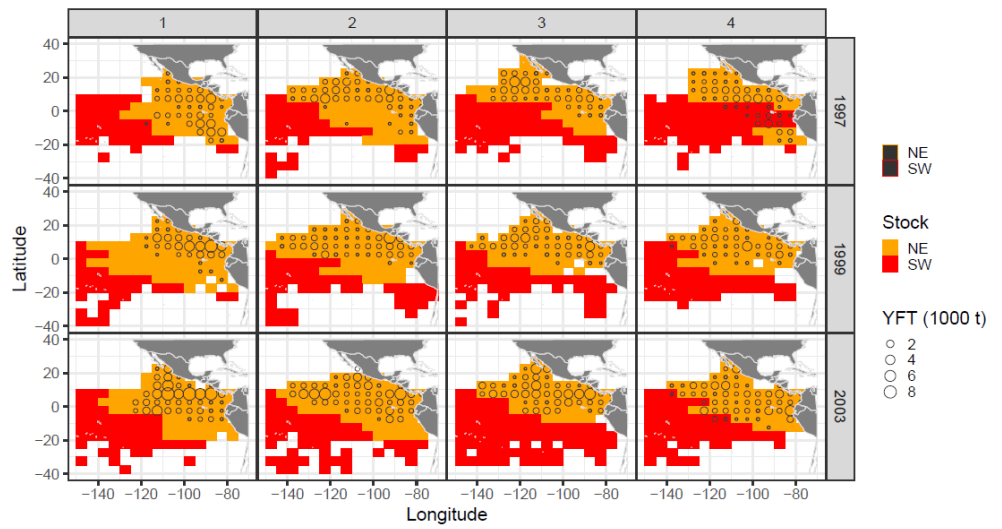


FIGURE 21. Distribution of purse seine catches on dolphin sets by quarter and year (1997 – El Niño, 1999 – La Niña, 2003 – Neutral) overlaid on the areas where catches of yellowfin occurred (all gears) classified as NE and SW .

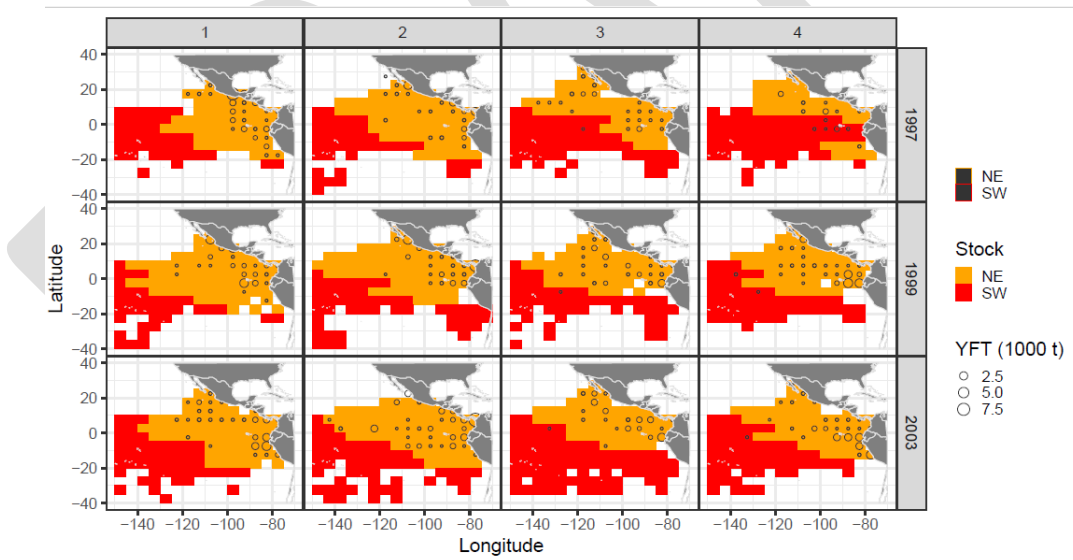


FIGURE 22. Distribution of purse seine catches on unassociated sets by quarter and year (1997 – El Niño, 1999 – La Niña, 2003 – Neutral) overlaid on the areas where catches of yellowfin occurred (all gears) classified as NE and SW.

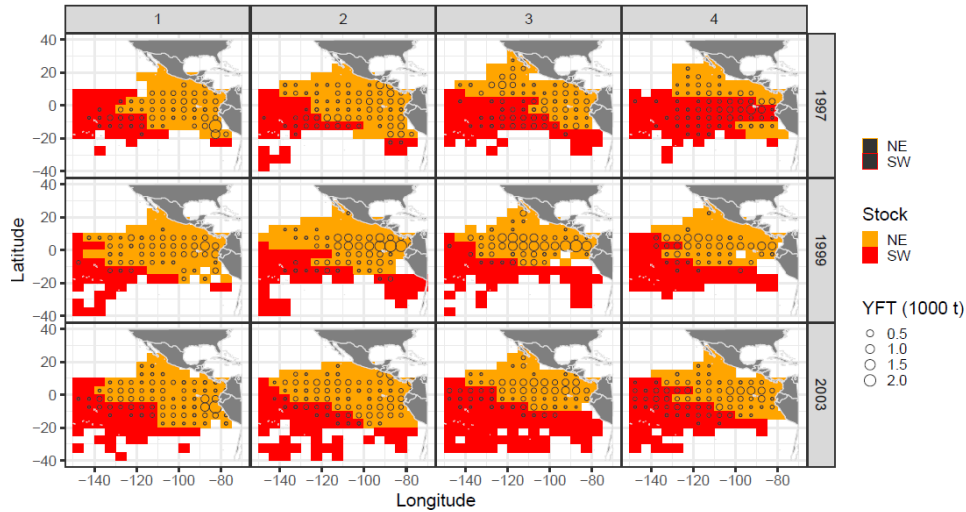


FIGURE 23. Distribution of purse seine catches on floating objects sets by quarter and year (1997 – El Niño, 1999 – La Niña, 2003 – Neutral) overlaid on the areas where catches of yellowfin occurred (all gears) classified as NE and SW.

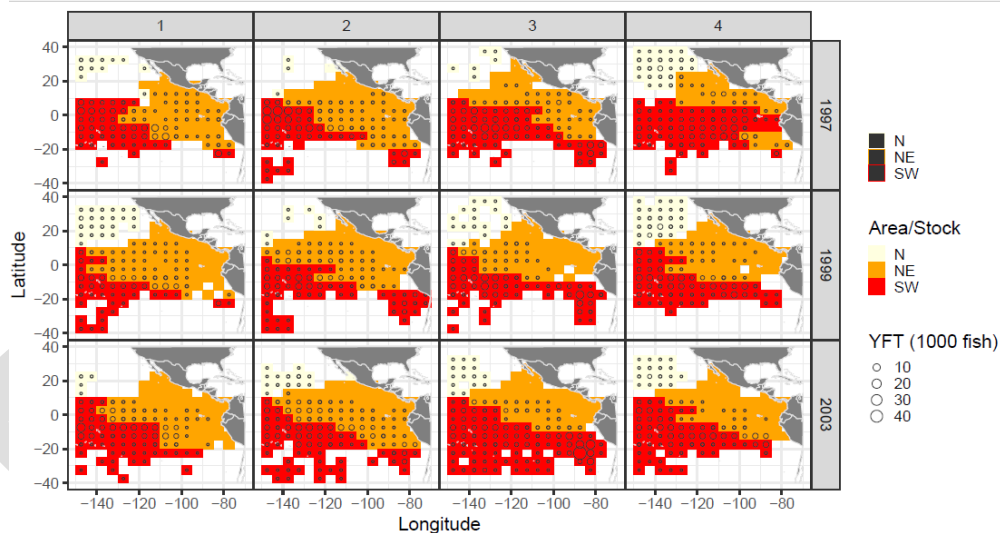


FIGURE 24. Distribution of longline catches (in numbers) from by quarter and year (1997 – El Niño, 1999 – La Niña, 2003 – Neutral) overlaid on the areas where catches of yellowfin occurred (all gears) classified as NE and SW, and the north (N) area.

Population trends and dynamics

A closer inspection of the contradictory indices of abundance available for yellowfin tuna in the EPO, the longline and the purse-seine associated with dolphins, points towards the alternate effect of El Niño and La Niña on the two populations. Indices based on the longline and purse-seine CPUE were standardized using spatiotemporal modelling in an attempt account for spatial effects (IATTC 2022). The associated length frequencies were also standardized (Maunder et al 2020). The spatial domain for both indices is disjoint (**Figure 25**) and coincide on average with the NE and SW areas defined previously and exclude the colder areas. The longline index encompasses the south EPO from about 90°W to the west with increasing latitudinal range from 90°W to 115°W, forming a diagonal from about 15°S to about 5°N. From 115°W to the west, areas in the northern and the southern hemisphere are included. The domain of the purse-seine

index is a triangle formed by the coast of the Americas, from 5°N to the Gulf of California, and lines from the coast to about 135°W and 10°N.

Even with the standardization, the inconsistencies among the two indices persisted (**Figures 26**). The mismatch was most apparent in 2001-2003, when a peak occurred earlier in the longline index and later in the purse-seine index (opposite to what was expected given the growth and selectivity assumptions of the assessment model, **Figure 26**). The standardized length frequencies showed that the 1998 cohort (coinciding with an important El Niño year) was prominent in the longline index and composed the peak in abundance two years later (**Figure 26**). That cohort was not seen in the purse-seine index. The opposite occurred with the 1999 cohort, which coincided with an equally important La Niña year (**Figure 25**).

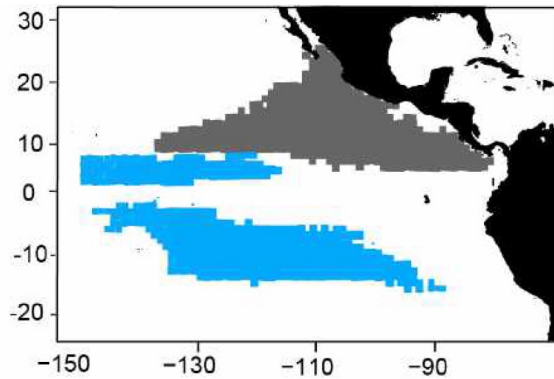


FIGURE 25. Spatial domain for the purse-seine (grey) and longline indices of abundance (blue).

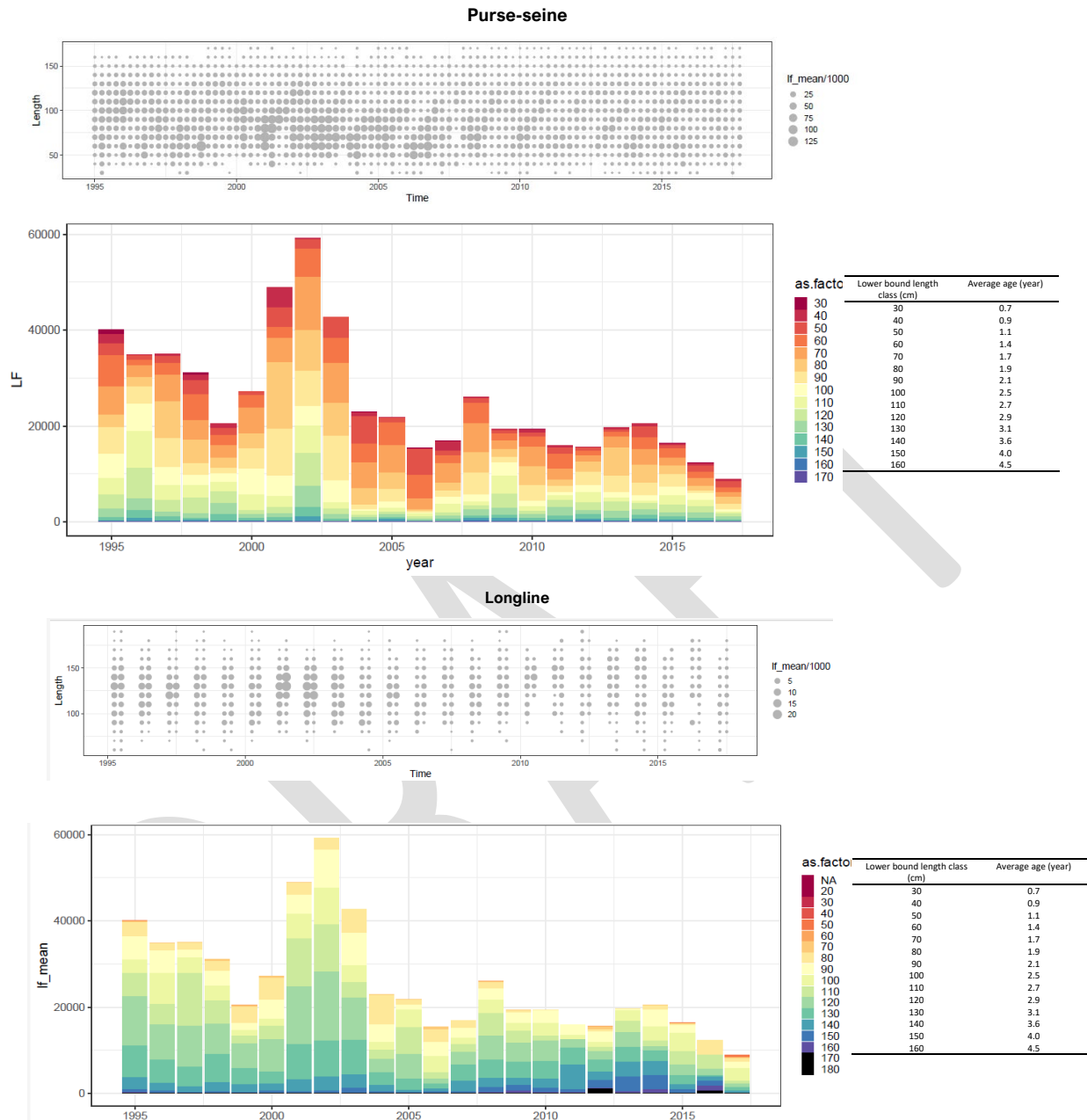


FIGURE 26. Purse seine (top) and longline (bottom) indices of abundance by length class and year. Quarter 2 was used for comparison to control for seasonal variations in the indices.

New longline indices of abundance were constructed by area. The Japanese longline data presents acceptable coverage of both areas only in quarters 1 and 2. For quarters 3 and 4, after 2001 the coverage declines substantially in the NE area.

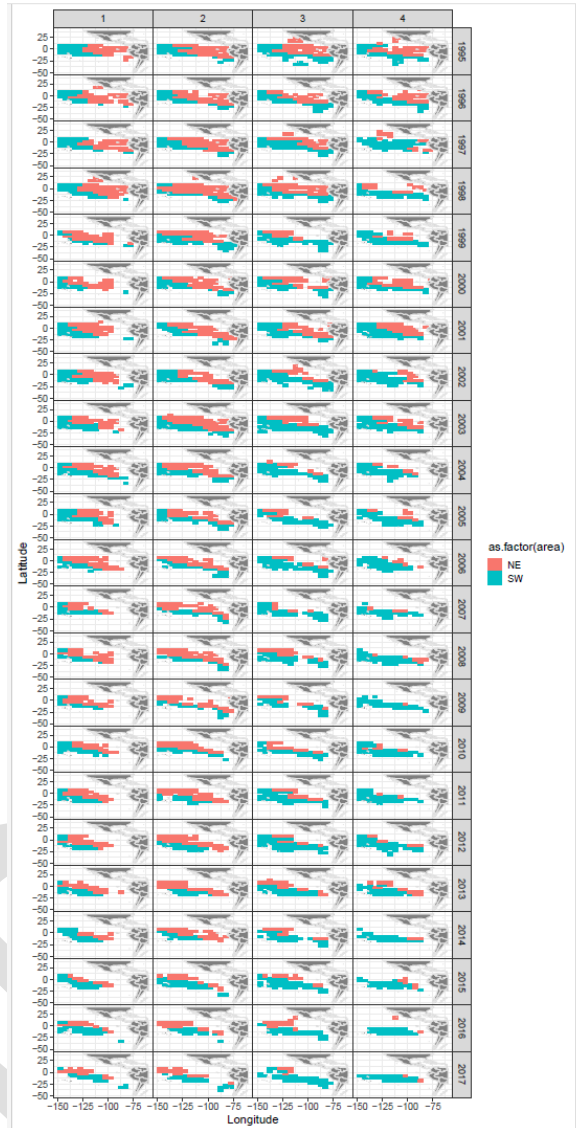


FIGURE 27. Spatial coverage of the Japanese longline fleet allocated to the two areas.

The indices of abundance derived from the longline data from the Japanese fleet for the two stocks (NE, SW) showed different trends. The SW index had the largest peak in year 2000, while the NE index had the largest peak in year 2001, closer to the peaks in the purse-seine index (year 2001 for quarter 2, 2002 for quarters 1,3,4) (**Figure 28**).

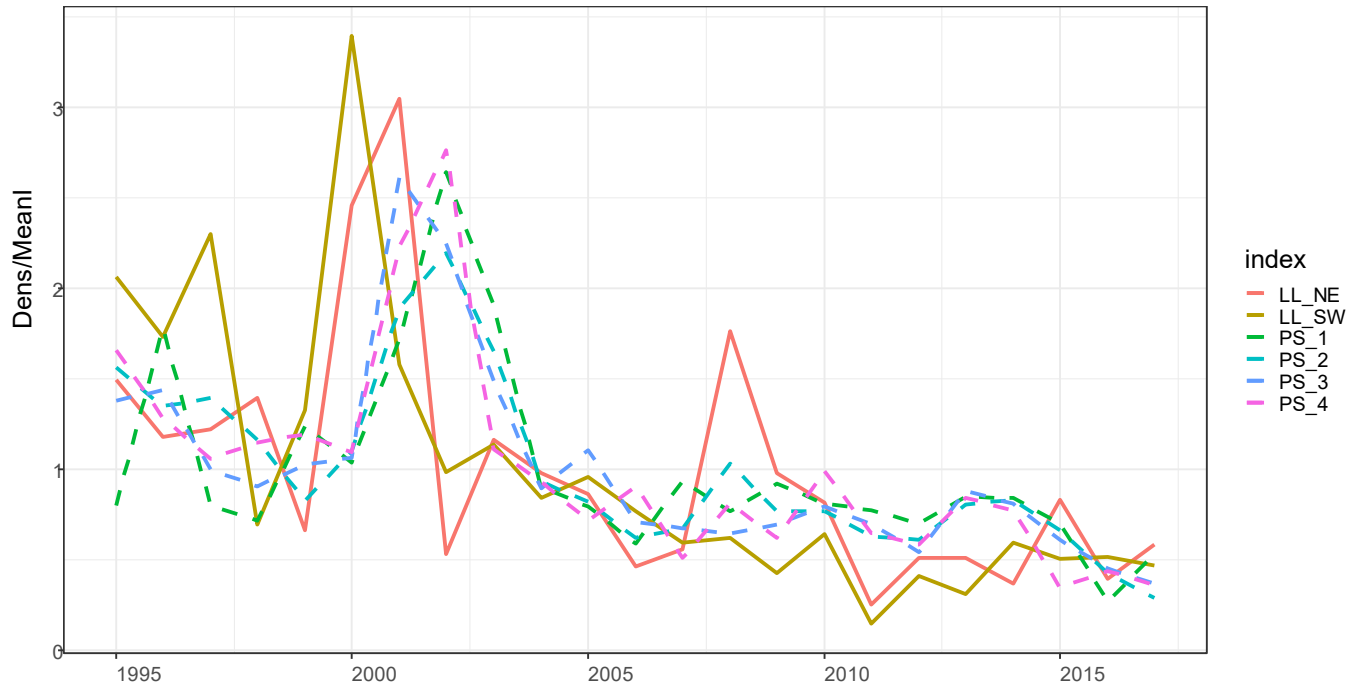


FIGURE 28. Index of abundance longline for NE and SW stocks (quarter 2) and comparison with the PS index for all quarters.

CATCHES

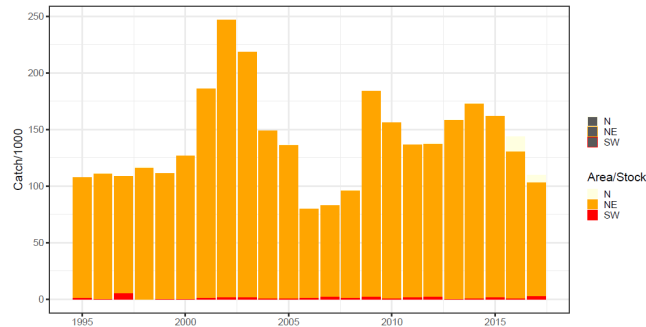
An estimate of the proportion of catches in the two stocks was obtained using the observer catch and effort data base for purse-seine ([BET-02-06](#)) and the longline catch data and using spatial information ([BET-02-03](#)). A rule for splitting the stock was based on the classification of each 5 x 5 cell by quarter and year either the NE or the SW area. In addition, a second rule was imposed. If there were discontinuous cells classified as the same stock in a 5-degree latitudinal band, the cell with the most western latitude was considered to be the location of the boundary. In addition, the longline catches not classified were assumed to come from the a “North” area if they were in the northern hemisphere or from the SW area if they came from the southern hemisphere.

The longline catches come mostly from the SW stock, while the purse-seine catches come mostly from the NE stock (**Figure 29, Table 2**). Almost all the dolphin-associated and unassociated purse-seine catches were caught in the NE. Of purse-seine catches associated with floating objects, 17% came from the SW, and the rest from the NE. For longline, it was the opposite, 17% came from the NE and 79% from the SW. Only small proportion of the longline and purse-seine catches comes from the north area.

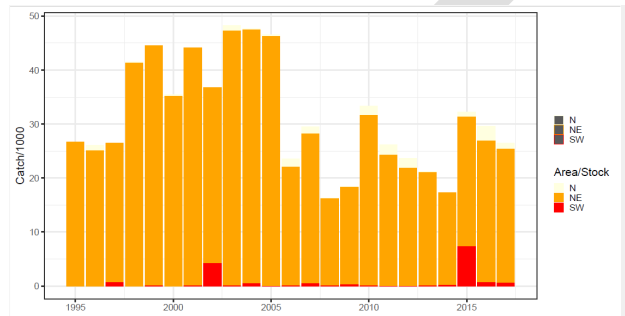
Table 2. Average proportion of the catches (in weight for purse-seine and in numbers for longline) from the NE and SE putative stocks and from the north area.

Gear	Set type	NE	SW	N
Purse-seine	Dolphin	99%	1%	1%
	Unassociated	96%	2%	2%
	Floating Objects	83%	17%	0%
Longline		17%	79%	4%

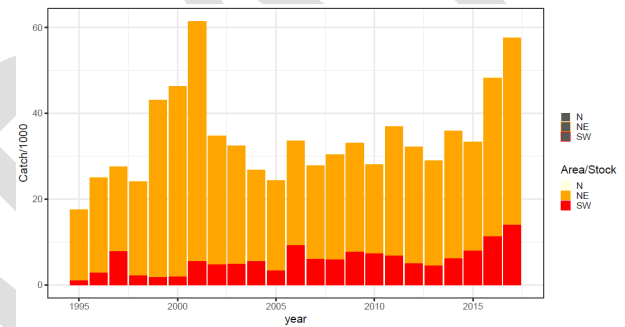
Dolphin set



Unassociated



Floating objects



Longline

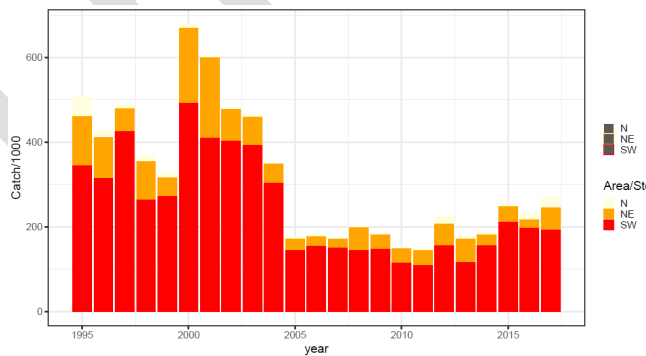


FIGURE 29. Yellowfin tuna catches by year and gear split by stock and area (1995-2017).. Purse-seine catches in 1,000 t, Longline catches in 1,000 fish.

DISCUSSION

The conceptual model for yellowfin tuna in the EPO summarizes the most up-to-date information available. The current understanding is that there are at least two stocks in the EPO. One stock located mainly in the coastal areas, extending into the northern hemisphere and well into oceanic waters. We refer to this as the NE stock. The other stock is located mainly in the southern hemisphere and may extend towards the CPO and towards the coast of Chile in the east depending on the oceanographic conditions. The area occupied by each stock in the EPO varies seasonally and interannually, as it is associated with major and distinct oceanographic features and biogeochemical provinces.

The NE stock is associated with the eastern tropical Pacific mesopelagic region and the SW stock is associated with the warm pool. Yellowfin tuna can spawn almost every day if the water temperatures are in the range of 24 to 30°C, resulting in year-round spawning in equatorial waters and seasonal spawning periods in areas farther from the equator (Nishikawa *et al.*, 1985; Schaefer 1998; Itano 2000, Schaefer and Fuller 2022). Due to the relative regional fidelity of yellowfin tuna movements and the widespread availability of habitat for spawning and larval development in the tropical regions of the EPO (productive waters above 24°C), it is hypothesized that yellowfin tuna in the Pacific Ocean may have evolved through isolation by distance. The fish from the NE stock would be adapted to the shallow thermocline and oxycline by associating with dolphins and birds. Yellowfin tuna in the NE would also benefit from the local depletion of bigeye tuna in that area, in case the food resources were limiting and shared between the two species because the thermocline is shallow and both species could forage efficiently in the mesopelagic zone. The fish in the SW stock would be more transient and moving to the extent that the warm pools extend. The yellowfin tuna in this area would coexist more frequently with bigeye tuna, although bigeye tuna would have advantages due to its adaptations for deep dives and because the mesopelagic zone is deeper. Patterns in the length frequency for purse-seine fisheries in all set types are consistent with the split in the NE and SW group (unpublished analysis).

Although the existence of at least two stocks seems clear and logical, the actual boundary of the stock is less clear. In this work, we used the length frequency of the floating object fishery to inform the boundary along the environmental gradient summarized in a principal component analysis on oceanographic variables. The resulting boundary clearly distinguished areas with different values for some oceanographic variables, such as temperature at 100 m, depth of the thermocline, and the oxycline, which are used to define different biogeochemical provinces. These areas are also consistent with the change in the oxycline, which in the NE stock is less than 50 m, while in the SW is at more than 200 m (**Figure 30**). In addition, this boundary delimits the area where the purse-seine on dolphins occurs, as almost all catches from this fishery are within the limits of the NE stock. This makes a strong case for that boundary. **Future work should focus on evaluating the implications of uncertainty in the boundary.**

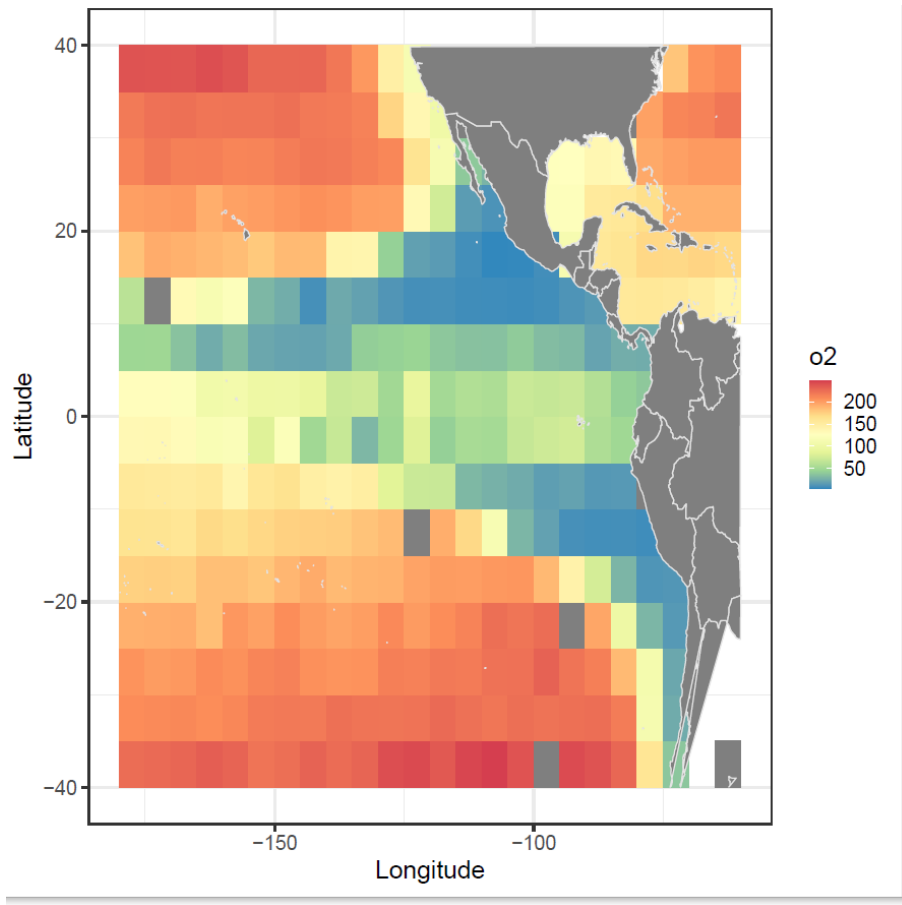


FIGURE 30. Average concentration of O₂ at 200 m from the word ocean atlas.

As hypothesized in the 2020 Benchmark assessment, this boundary may be a “porous” one and some mixing may exist. Ideally, the tagging program should provide important information about the movement between the two stocks and the net rate of movement between them. In the Pacific Ocean, output of the SEAPODYM⁴ model has been used to inform movements between areas for the stock assessments of yellowfin, bigeye and skipjack tuna, as alternative to the actual tagging data. **In the future, exploring the movement rates from tagging data and from ecosystem models such as SEAPODYM should be explored.**

The staff believes the method proposed here may be used to split the two stocks. However, the boundaries are plastic and dynamic, changing seasonally and interannually. This may complicate the estimation of the purse-seine catches and corresponding length composition data using port sampling data, at least for unassociated and floating object catches even though the scale of the boundary is in 5° of latitude and 5° of longitude. The catches of the purse-seine associated with dolphins should all be included in the NE, given the conceptual model. **Future studies should focus on either facilitating the catch estimation for those two set types, in a dynamic way, or evaluating the consequences of fixing the boundaries to an average for all years or by type of condition (El Niño, La Niña, and Neutral).**

Length frequencies for all set types also indicate the effect of the California current in the north, and the Humboldt current in the south. We hypothesize that the area of influence of those two currents would be important feeding areas, due to their high productivity, rather than spawning areas as the conditions of

⁴ SEAPODYM is a basin-scale ecosystem-linked population models of large pelagic predators forced by oceanographic variables

temperature above 24°C occur only seasonally. Archival tagging data show that yellowfin in the California current may move towards warmer areas during their lives. We further assume that those two areas are part of the NE stock. However, isolation by distance may also play a role and local depletions may be important. For simplicity, the two areas should be considered in a model for the NE stock as “areas-as-fleet” and the availability of different sizes modelled using selectivity curves. **Future studies should focus on comparing the length frequencies of fixed fishery definitions versus dynamic fishery definition to evaluate the trade-off between realism and practicality, as for the catch estimation.**

The NE area is an area where large yellowfin tuna may occur in higher density. Most of the catches of yellowfin tuna in the EPO are taken from this area and it should be the focus of assessment and management. The assessment of the NE stock may follow closely the same methods as the 2020 Benchmark Assessment. It seems that there is a lot of information about abundance in the fishery data through the ability of the models to follow the depletion of the cohorts exploited first by the floating object fisheries, when young and small, then caught by the purse-seine fishery on dolphins, when larger and older. A depletion estimator seems to be able estimate the biomass and it is consistent with the length composition data (Minte-Vera et al, 2021). **Future studies should refit the depletion model to the data from the purse-seine fishery occurring only in the NE area.** In addition, there is a purse-seine index based on the dolphin sets and was the main index of abundance used in the 2020 Benchmark Assessment. **Future work should focus on improving the index of abundance for the dolphin associated fishery.**

The SW stock is mainly in areas with higher abundance of bigeye tuna. It is exploited by purse-seine on floating objects and by longline fisheries, which are also the main fisheries for bigeye tuna. The assessment for the SW stock may have to be done in collaboration with SPC, similarly to what is done for the south Pacific albacore tuna ([SAC-13-INF-S](#)). For example, an index of abundance for the CPO could be investigated for similarities with the SW index; the EPO catches could be added in one of the sensitivity models for the stock assessment of the WCPO stock. For management, the stock status from the WCPO assessment should be monitored. Another interim option be to associate the management with bigeye tuna in the EPO, since the yellowfin tuna SW stock is likely more productive than bigeye tuna, and both species may have similar vulnerability in that area as they are exploited by the same fisheries there (purse-seine on floating objects and longline). Managing those fisheries (e.g. reducing the number of FADs, reducing the number of FAD sets, catch limits on bigeye tuna) would likely benefit both species (because of the similarities in preferable habitat of this species in this area). **For now, the options are to monitor it using indicators such as the longline index of abundance of the stock in the EPO and the standardized length composition corresponding to the index**, which are already included in the stock status indicator document ([SAC-14-04](#)).

Finally, understanding the processes behind the population dynamic patterns will not only help the staff improve stock assessment models but also allow for the construction of models that can adapt to environmental changes and changes in the fleet.

FUTURE DIRECTIONS

In preparation for the benchmark assessment, the points raised in the discussion section above will be addressed. In addition, the recommendations from the previous [external review panel](#) and the review panel planned for 2023 will be taken into account, as well as the lessons learnt on the recent [CAPAM workshops](#). Specifically, the staff plans to focus on:

Collection of new and updated information

- a. Continue its collection and analysis of purse-seine data (catch, effort, and size-composition)
- b. Continue collaborative work with longline CPCs
- c. Continue tagging and biology studies and analyses

Refinements to the assessment model and methods

- a. Address uncertainty in spatial/stock structure
- b. Continue research on CPUE and length-frequency standardization methods
- c. Work with purse-seine CPCs to understand changes in fishing strategies to inform selectivity modelling
- d. Continue exploring uncertainty in growth and selectivity
- e. Explore uncertainty in natural mortality
- f. Explore different stock assessment time spans, initial conditions and types of models (monthly/weekly models, depletion models)

REFERENCES

- Anderson, G., Lal, M., Hampton, J., Smith, N., and Rico, C. 2019. Close kin proximity in yellowfin tuna (*Thunnus albacares*) as a driver of population genetic structure in the tropical western and central Pacific Ocean
- Bernal, D., Brill, R.W., Dickson, K.A., Shiels, H.A. 2017. Sharing the water column: physiological mechanisms underlying species-specific habitat use in tunas. *Rev Fish Biol Fisheries* 27:843–880
- Díaz-Jaimes, P., and Uribe-Alcocer, M. 2006. Spatial differentiation in the eastern Pacific yellowfin tuna revealed by microsatellite variation. *Fisheries Science* 2006 (72): 590–596.
- Dickson, J.M., and Dickson, K.A. 2019. Ontogenetic change in the amount and position of slow oxidative myotomal muscle in relationship to regional endothermy in juvenile yellowfin tuna *Thunnus albacares*. *J. Fish. Biol.* 95: 940–951.
- Estes, D. H. 1983. Shio-Japanese pioneers in San Diego's Fishery. In: *Boat and Ship building in San Diego; 11th Annual Cabrillo Festival Historic Seminar*. San Diego California, Cabrillo Historical Association. 1: 25-43.
- Fiedler, P.C., and Talley, L.D. 2006. Hydrography of the eastern tropical Pacific: A review. *Progress in Oceanography* 69: 143–180.
- Grewe, P., Hampton, J. 1998. An assessment of bigeye (*Thunnus obesus*) population structure in the Pacific Ocean, based on mitochondrial DNA and DNA microsatellite analysis. CSIRO Marine Research, Hobart, Australia.
- Lennert-Cody, C.E., and Tomlinson, P.K. 2010a. Evaluation of aspects of the IATTC port sampling design and estimation procedures for tuna catches. *Inter-Amer. Trop. Tuna Comm., Stock Assessment Report*, 10: 279-309.
- Lennert-Cody, C.E., Minami, M., Tomlinson, P.K., Maunder, M.N. 2010b. Exploratory analysis of spatial-temporal patterns in length-frequency data: An example of distributional regression trees. *Fisheries Research* 102: 323-326
- Lennert-Cody, C.E., Maunder, M.N., Aires-da-Silva, A., and Minami, M. 2013. Defining population spatial units: Simultaneous analysis of frequency distributions and time series. *Fisheries Research* 139: 85-92.
- Longhurst, A. 2007. *Ecological Geography of the Sea*, Academic Press, London
- Maunder, M.N., Punt, A.E. 2013. A review of integrated analysis in fisheries stock assessment. *Fisheries Research* 142: 61-74
- Maunder, M.N. and Watters, G.M. 2003. A-SCALA: an age-structured statistical catch-at-length analysis for assessing tuna stocks in the eastern Pacific Ocean. *IATTC Bull.* 22: 433-582.
- Maunder, M.N., Deriso, R.B. 2013. A stock–recruitment model for highly fecund species based on temporal and spatial extent of spawning. *Fisheries Research* 146: 96– 101.
- Maunder, M.N., Thorson, J.T., Xu, H., Oliveros-Ramos, R., Hoyle, S.D., Tremblay-Boyer, L., Lee, H.H., Kai, M., Chang, S.-K., and Kitakado, T. 2020b. The need for spatio-temporal modeling to determine catch-per-unit effort based indices of abundance and associated composition data for inclusion in stock assessment models. *Fisheries Research* 229: 105594

- Minte-Vera, C.V., Maunder, M.N., Aires-da-Silva, A.M. 2021. Auxiliary diagnostic analyses used to detect model misspecification and highlight potential solutions in stock assessments: application to yellowfin tuna in the eastern Pacific Ocean. *ICES Journal of Marine Science* 78 (10): 3521– 3537
- Monterey, G.I.; Levitus, S. 1997. Seasonal variability of mixed layer depth for the world ocean: US Department of Commerce, National Oceanic and Atmospheric Administration United States. National Environmental Satellite, Data. NOAA Atlas NEDIS 14.
<https://repository.library.noaa.gov/view/noaa/49153>
- Muñoz-Abril, L., Torres, M. de L., Valle, C. A, Rubianes-Landazuri, F. Galván-Magaña, F., Canty, S. W. J, Terán, M.A., Brandt, M., Chaves, J.A., Grewe, P.M., 2022. Lack of genetic differentiation in yellowfin tuna has conservation implications in the Eastern Pacific Ocean. *PLoS ONE* 17(8): e0272713.
<https://doi.org/10.1371/journal.pone.0272713>
- Nishikawa, Y., Honma, M., Ueyanagi, S., Kikawa, S. 1985. Average distribution of larvae of oceanic species of scombrid fishes, 1956–1981. *Far Seas Fisheries Research Laboratories S Series* 12, 1–99.
- Pecoraro, C., Babbicci, M., France, R., Rico, C., Papetti, C., Chassot, E., Bodin, N., Cariani, A., Bargelloni, L., Tinti, F. 2018. The population genomics of yellowfin tuna (*Thunnus albacares*) at global geographic scale challenges current stock delineation. *Scientific Reports* 8, 13890.
- Reygondeau, G., Guidi, L., Beaugrand, G., Henson, S.A., Koubbi, P., MacKenzie, B.R., Sutton, T.T, Fioroni, M., Maury, O. 2017. Global biogeochemical provinces of the mesopelagic zone
- Reygondeau, G., Longhurst, A., Martinez, E., Beaugrand, G., Antoine, D., Maury, O. 2013. Dynamic biogeochemical provinces in the global ocean. *Global Biogeochemical Cycles* 27: 1046–1058
- Rooker, J.R., Wells, R.J.D., Itano, D.G., Thorrold, S.R., Lee, J.M. 2016. Natal origin and population connectivity of bigeye and yellowfin tuna in the Pacific Ocean. *Fish. Oceanogr.* 25(3): 277-291.
- Schaefer, K.M., Fuller, D.W., 2022. Spatiotemporal variability in the reproductive biology of yellowfin tuna (*Thunnus albacares*) in the eastern Pacific Ocean. *Fisheries Research* 248: 106225.
<https://doi.org/10.1016/j.fishres.2022.106225>
- Schaefer, K.M. 1998. Reproductive biology of yellowfin tuna (*Thunnus albacares*) in the eastern Pacific Ocean. *Inter-Amer. Trop. Tuna Comm., Bull.* 21: 203-272.
- Schaefer, K.M. 2009. Stock structure of bigeye, yellowfin, and skipjack tunas in the eastern Pacific Ocean. IATTC Stock Assessment Report, 9, Status of the tuna and billfish stocks in 2007: 203-221.
<http://www.iattc.org/PDFFiles2/StockAssessmentReports/SAR9-Stock-Structure-SPN.pdf>
- Schaefer, K.M., Fuller, D.W., and Block, B.A. 2007. Movements, behavior, and habitat utilization of yellowfin tuna (*Thunnus albacares*) in the northeastern Pacific Ocean, ascertained through archival tag data. *Mar. Biol.*, 105: 503-525.
- Schaefer, K.M., Fuller, D.W., and Block, B.A. 2011. Movements, behavior, and habitat utilization of yellowfin tuna (*Thunnus albacares*) in the Pacific Ocean off Baja California, Mexico, determined from archival tag data analyses, including Kalman filtering. *Fish. Res.* 112, 22-37.
- Schaefer, K.M., Fuller, D.W., and Aldana, G. 2014. Movements, behavior, and habitat utilization of yellowfin tuna (*Thunnus albacares*) in waters surrounding the Revillagigedo Islands Archipelago Biosphere Reserve, Mexico. *Fish. Ocean.* 23: 65-82.
- Schaefer, K.M., Fuller, D.W. 2021. Horizontal movements, utilization distributions, and mixing rates of yellowfin tuna (*Thunnus albacares*) tagged and released with archival tags in six discrete areas of the eastern and central Pacific Ocean. *Fisheries Oceanography*. 2021;1–24.

- Scott, M.D., Chivers, S.J., Olson, R.J., Fiedler, P.C., Holland, K. 2012. Pelagic predator associations: tuna and dolphins in the eastern tropical Pacific Ocean. *Marine Ecology Progress Series* 458: 283-302.
- Suter, J.M. 2010. An evaluation of the area stratification used for sampling tunas in the eastern Pacific Ocean and implications for estimating total annual catches. [IATTC Special Report 18](#).
- Sutton, T.T, Clark, M.R., Dunn, D.C., Halpin, P.N., Rogers, A. D., Guinotte, J., Bograd, S.J., Angel, M.V., Perez, J.A.A, Wishner, K., Haedrich, R.L., Lindsay, D.J., Drazen, J.C, Vereshchakam, A., Piatkowskin, U. Morato, T., Błachowiak-Samołyk, K., Robison, B.H., Gjerder, K.M., Pierrot-Bults, A., Bernal, P., Reygondeau, G., Heino, M. 2017. A global biogeographic classification of the mesopelagic zone. *Deep-Sea Research Part I* 126: 85–102.
- Suzuki, Z., Tomlinson, P.K. Honna, M.1978. Population structure of Pacific yellowfin tuna. *Bulletin of the Inter-American Tropical Tuna Commission Stock Assessment* 17 (5): 277-441.
- Thorson, J.T., and Barnett, L.A.K. 2017. Comparing estimates of abundance trends and distribution shifts using single- and multispecies models of fishes and biogenic habitat. *ICES Journal of Marine Science* 74(5): 1311-1321.
- Thorson, J.T., and Haltuch, M.A. 2018. Spatiotemporal analysis of compositional data: increased precision and improved workflow using model-based inputs to stock assessment. *Canadian Journal of Fisheries and Aquatic Sciences* (999): 1-14.
- Tomlinson, P.K. 2002. Progress on sampling the eastern Pacific Ocean tuna catch for species composition and length-frequency distributions. *Inter-Amer. Trop. Tuna Comm, Stock Assess. Rep. 2*: 339-365.
- Ward RD, Elliott NG, Innes BH, Smolenski AJ, Grewe PM. 1997. Global population structure of yellowfin tuna, *Thunnus albacares*, inferred from allozyme and mitochondrial DNA variation. *Fish. Bull.* 1997 (95): 566–575.
- Ward, R. D., Elliott, N. G., Grewe, P. M., and Smolenski, A. J. 1994. Allozyme and mitochondrial DNA variation in yellowfin tuna (*Thunnus albacares*) from the Pacific Ocean. *Marine Biology* 118: 531–539.
- Waterhouse, L., Sampson, D.B., Maunder, M., Semmens, B.X. 2014. Using areas-as-fleets selectivity to model spatial fishing: asymptotic curves are unlikely under equilibrium conditions. *Fisheries Research* 158:15-25
- Wells, R.J., Rooker, J.R., and Itano, D.G. 2012. Nursery origin of yellowfin tuna in the Hawaiian Islands. *Mar. Ecol. Prog. Ser.* 461: 187-196.
- Wild, A. 1986. Growth of yellowfin tuna, *Thunnus albacares*, in the eastern Pacific Ocean based on otolith increments. *Inter-Amer. Trop. Tuna Comm. Bull.* 18: 421-482.
- Xu, H., Lennert-Cody, C.E., Maunder, M.N., and Minte-Vera, C.V. 2019. Spatiotemporal dynamics of the dolphin-associated purse-seine fishery for yellowfin tuna (*Thunnus albacares*) in the eastern Pacific Ocean. *Fish. Res.* 213: 121-131.

APPENDIX A. PRINCIPAL COMPONENT ANALYSIS ON OCEANOGRAPHIC VARIABLES

To discriminate the epipelagic provinces sea surface temperature (SST), sea surface salinity (SAL) and chlorophyll a concentration (CHL_a) have been used (Reygondeau et al, 2013). In addition to temperature and salinity, oxygen at depth nutrient concentrations (NO₃, SiO₂, PO₄) and flux of particulate organic carbon has been used to discriminate the mesopelagic provinces (Sutton et al 2017, Reygondeau et al (2017). Those variables, however, are only available as average values that result from integration of many data sources (“climatology”) and are not amenable for dynamic analysis.

For this study, data from the purse-seine fisheries coupled from oceanographic variables compiled from a previous project was used (SAC-10-Inf-D). The data available was from 1995 to 2017 of the positions of each set was taken from the observer catch and effort database obtained from the AIDCP observer program. Information on surface and subsurface variables were matched to each set, regardless of set type and catch composition. The surface variables chosen were sea surface temperature (SST), salinity (SAL), sea surface height (SSH), eddy kinetic energy (EKE) and the subsurface variables chosen were sea temperature at 100 m (SST_100), isothermal layer depth (ILD) and mixed layer depth (MLD). The ILD provides an index of the depth of the surface mixing. The ILD was calculated as the depth corresponding to a 0.5°C temperature difference relative to the sea surface temperature (Monterey and Levitus 1997, SAC-10-Inf-D). For some years, the concentration of Chlorophyll a and a frontal index were available (SAC-10-Inf-D), but were not used because that would reduce the data set to about 2/3 of the size.

Each variable was aggregated to a “cell” of a 5°latitude by 5°longitude by quarter by obtaining the median for all sets in that cell. The variables were centered to the overall median and were divided by the interquartile range (quantile of 90% - quantile of 10%) so that all were in the same scale. A principal component analysis was used to summarize the variables. The maps of the principal components 1 and 2 were plotted by year and quarter to inspect where a dynamic boundary between the two stocks may lay.

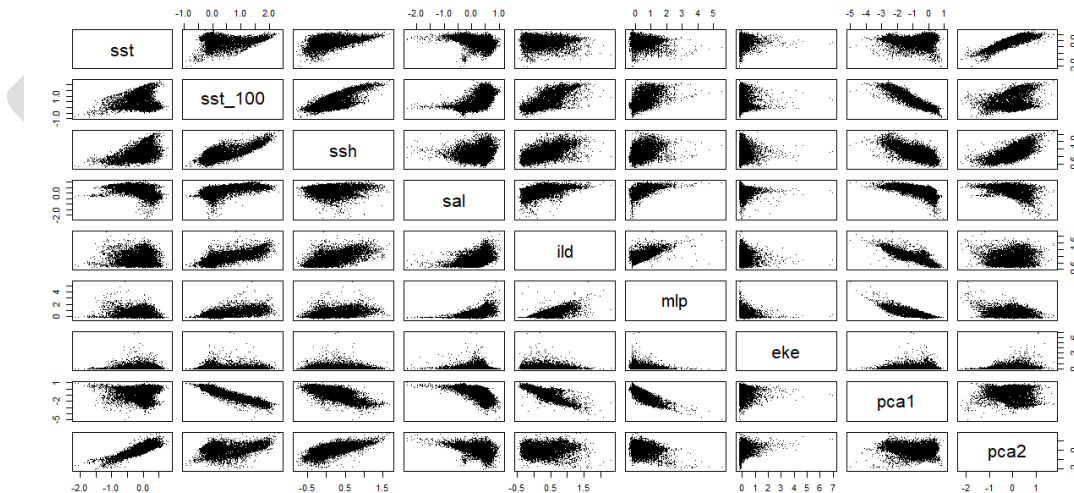


FIGURE A1. Scatterplot of the environmental variables (surface variables: sea surface temperature (SST), salinity (SAL), sea surface height (SSH), eddy kinetic energy (EKE); subsurface variables: sea temperature at 100 m (SST_100), isothermal layer depth (ILD) and mixed layer depth (MLD)) and the first two principal components (pca1,pca2)

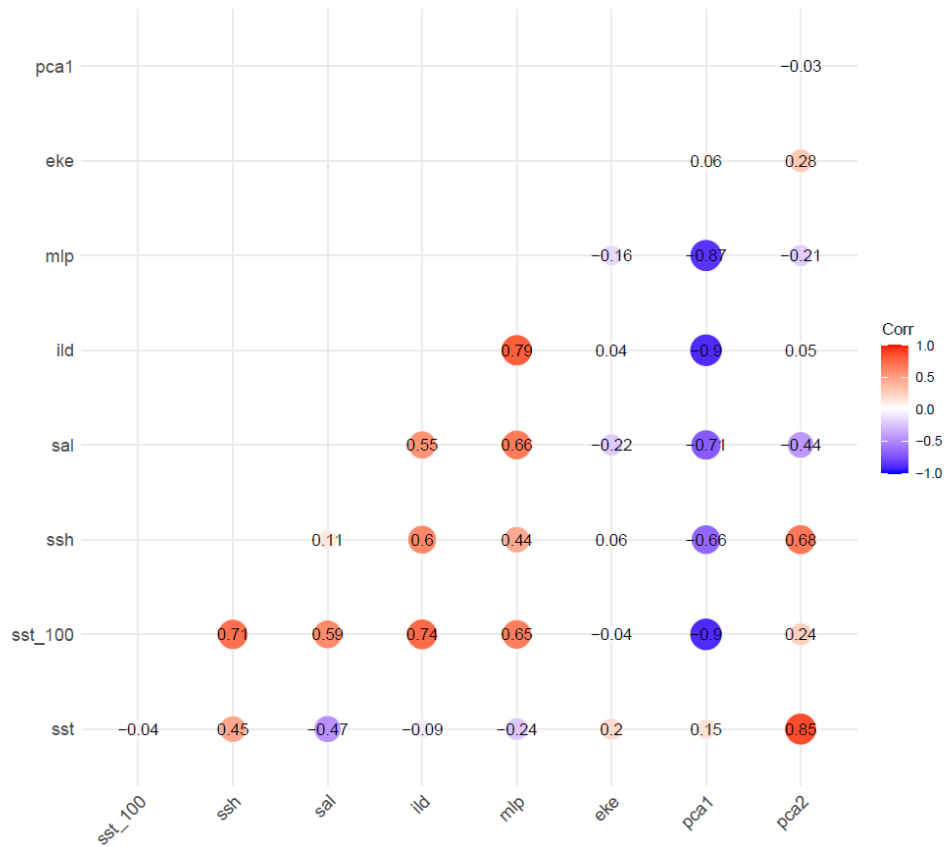


FIGURE A2. Pearson correlations between the environmental variables and the first two principal components. variables (surface variables: sea surface temperature (SST), salinity (SAL), sea surface height (SSH), eddy kinetic energy (EKE); subsurface variables: sea temperature at 100 m (SST_100), isothermal layer depth (ILD) and mixed layer depth (MLD)) and the first two principal components (pca1, pca2).

APPENDIX B. REGRESSION TREE ANALYSIS ON LENGTH-FREQUENCY DATA

The length-frequency data for the purse-seine fisheries are obtained through the sampling program conducted by IATTC personnel at ports of landing in Ecuador, Mexico, Panama, and Venezuela. The ancillary information available in the port-sampling database is determined by the governing protocol (Tomlinson 2002, Suter 2010), which specifies the strata from which samples are collected: fish-carrying capacity of the vessel, type of set (DEL, NOA, OBJ), month and area of catch (13 areas; see Figure 1 in [WSBET-02-06](#)). Wells are the primary sampling unit within a stratum, with unequal numbers of wells sampled per stratum, and fish within a well are the secondary sampling unit. Sampling at both stages is largely opportunistic, except that a well is sampled only if all the catch within it came from the same stratum. This restriction can result in sets with large catches predominating in the samples (Lennert-Cody and Tomlinson 2010a). More than one well may be sampled per vessel if the catch in the other wells comes from different strata, but typically only one or two wells per trip are sampled. For large and small purse-seine vessels, about 50%-60% and 10-20% of trips, respectively, have typically been sampled per year, for a total of over 800 wells sampled in most years (IATTC 2010a; Vogel 2014). The sampling coverage in terms of percentage of the catch is lower (SAC-02-10). The sampling areas were designed for yellowfin prior to the development of the fishery on FADs. Since 2000, both the 5° cell and the sampling area have been recorded for almost all samples (Lennert-Cody et al. 2012); the 5° cell has been recovered for many samples prior to 2000. Ideally, 50 fish of each species in the sampled well were measured, and since 2000 samplers alternate between counting fish by species and measuring fish for length. The protocol varies to some extent with the set type associated with the catch in the well and with the species composition of the catch in the well, as recorded by the observer or in the vessel's logbook. More details on the port sampling program can be found in the Appendix of Suter (2010) and in [WSBET-02-06](#). The data used in this analysis is raised to the well level.

A regression tree approach was used for analyzing length frequency data. The regression tree algorithm (Lennert-Cody *et al.* 2010b, Lennert-Cody *et al.* 2013) uses recursive partitioning to search for hierarchical binary decision rules that divide the data into more homogeneous subgroups. The binary decision rules are selected to provide the greatest decrease in the heterogeneity of length composition data, which is measured based on the Kullback–Leibler divergence. The regression tree algorithm has been recently included in an R package *FishFreqTree* (<https://github.com/HaikunXu/FishFreqTree>, by Haikun Xu). The explanatory variables that can be used are latitude, longitude, quarter, cyclical-quarter, and year. In the current application, two environmental gradients summarized in a principal component analysis instead of latitude and longitude, thus each set was positioned along the environmental axes rather than in space.

The multivariate response variable for the regression tree was the length frequency data binned in 15 length classes as 0-20 cm, 20-30 cm, 30-40 cm, 40-50 cm, 50-60 cm, 60-70 cm, 70-80 cm, 80-90 cm, 90-100 cm, 100-110 cm, 110-120 cm, 120-130 cm, 130-140 cm, 140-150 cm and >150cm. The temporal predictors used were quarter (1,2,3,4) and cyclic quarter (4,1,2,3). The spatial predictors used by Lennert-Cody *et al.* (2013), latitude and longitude, were not used, instead the first two principal components were used as “spatial” predictors. The values were rounded to the nearest 0.05. The growth in length within a quarter was ignored as it is expected that the 10cm bin size class will encompass most of the growth within a quarter (it is expected that on average yellowfin tuna will grow about 3.5 cm per month when the growth is the fastest given the fixed growth function (SAC-12-06, Wild 1986). Also, the length composition was not corrected for the effect of recruitment (e.g. SKJ) as the timing of recruitment within a year could also be an indication of stock structure.

APPENDIX C. SPATIOTEMPORAL MODELS FOR CPUE STANDARDIZATION

Purse seine index: The data used to construct the index are the set-by-set catch and effort observations from purse-seine vessels. On-board observers of the Agreement on the International Dolphin Conservation Program (AIDCP) have been collecting these data for large purse-seine vessels (fish-carrying capacity >363 t) since 1992 (Scott *et al.* 2016). Logbook data were used for previous trips by such vessels, for which no observer data were available.

Because it is not possible to separate searching effort by set type, and to limit the data used to standardize effort to vessels that fish preferentially for dolphin-associated tuna, the following procedure was used to limit the standardization to the main dolphin-associated fishing grounds and vessels. Only data for 1°x1° sampling cells north of 5°N with at least 30 years of data during 1985-2019 were included, and only vessels that made at least 75% of their sets on dolphin-associated tunas during at least 10 of 18 years of data coverage were selected. The 52 selected vessels were classified as “dolphin-associated vessels”, and their data were used to obtain the index (see SAC-11-06 Appendix 1, Figure A1).

Longline index:

The CPUE data for the standardization of longline indices of abundance are collected from Japanese commercial longline vessels. Catch and effort are recorded in number of fish and number of hooks, respectively, and CPUE is computed as the number of fish caught per 1,000 hooks. The dataset is aggregated at a resolution of 1° cell x month x vessel x HBF and has been available since 1979. To address the concern that the westward contraction of the fishing ground in the past decade may result in biased index of abundance, we only select the CPUE data from the “core” longline fishing ground, which includes all 1° x 1° cells with at least 80 quarters of CPUE data between 1979 and 2019.

C1. Standardization procedure

The standardization of the catch and effort data was conducted using the R library *VAST* (version 3.0.0) (Thorson and Barnett 2017, Xu *et al.* 2019, Maunder *et al.* 2020b). *VAST* fits a delta-generalized linear mixed-effects spatiotemporal model to data. It models separately the encounter probability and positive catch rate, which are assumed to have a logit and log link, respectively, and combines the results to produce the final estimates. There are several advantages of using mixed-effects spatiotemporal models over the fixed-effects generalized linear models conventionally used in CPUE standardization. First, the estimation of spatiotemporal correlations allows for the prediction of catch rates in unfished locations based on the information from neighboring areas/times. Second, the uncertainty estimates take into consideration the spatial coverage and sample size. Third, the final estimates are naturally weighted by the area related to each knot in the spatial domain, rather than by the sample size. Both the encounter probability and the catch rates are modeled with linear predictors that include an intercept term (year-quarter effect), vessel effects on catchability and spatial effect (Xu *et al.* 2019). The spatial effect is represented by a mesh of 200 knots. The model converged (gradient = 0.0004) with a positive definite Hessian

The length frequencies of yellowfin associated with the index of abundance (“survey”) were also obtained from the standardization of the data from the dolphin-associated purse-seine fishery using *VAST*, with the inclusion of a multivariate response variable (Thorson and Haltuch 2018, Maunder *et al.* 2020b). The data used were the length frequencies collected by the port-sampling program. The length frequencies, raised to the well catch, were aggregated by quarter, 5° cell and set type. The aggregated data were raised to the catch in a stratum using data from the observer and logbook databases. Strata were defined as quarter-5° cell combinations. The vessel and spatial cell selection criterion was the same as the CPUE. The multivariate response variable was length-specific catch rate (in ton day⁻¹ fished). The length frequency

classes were defined by 10 cm intervals, from 20 to 190 cm.

The standardization model treats the encounter probability and positive catch rate separately, with logit and log links, respectively. The linear predictors are spatial and the temporal (year-quarter) components. The spatial component is represented by 30 spatial knots (that aggregate the 5° cells to improve computational efficiency). The sum of the indices by length class were similar to the overall index (section 2.3), indicating that the standardized length frequencies are a good representation of the length classes represented in the index of abundance. The model converged (gradient = 0.000006) with a positive definite Hessian. The classes with largest frequencies ranged from 40 to 160 cm with most lengths between 70 and 120.

The spatial domain for the purse-seine index associated with dolphins was allocated to NE, SW or north (Figure C1). The density for each area was obtained. Most of the index is allocated to the NE area, making this index and index for that area.



FIGURE C1. Allocation of the spatial domain of the purse-seine index associated with dolphins to the areas defined in this document.